Design Model for Bolted Moment End Plate Connections using Rectangular Hollow Sections

A. T. Wheeler, B.E.
M. J. Clarke, B.Sc., B.E., Ph.D.
G. J. Hancock, B.Sc., B.E., Ph.D.
T. M. Murray, B.S., M.S., Ph.D.

June 1997

Centre for Advanced Structural Engineering
Department of Civil Engineering
University of Sydney, N.S.W., Australia, 2006

Abstract

The report presents a model for the determination of the ultimate moment capacity of bolted moment end plate connections utilising rectangular hollow sections and two rows of bolts. The model considers the combined effects of prying action due to flexible end plates and the formation of yield lines in the end plates, enabling the design of the connection with a row of bolts above and below the section.

The model has been calibrated and validated using experimental data from an associated test program. The design model constitutes a relatively simple method for predicting the ultimate moment capacity for the particular type of bolted moment end plate connection described herein.

Table of Contents

1. Introduction

The increase in the use of rectangular hollow sections in mainstream structures coupled with the economics of prefabrication has highlighted the need for simple design methods that produce economical connections for tubular members. In an effort to address this need, the Australian Institute of Steel Construction (AISC) has published the document *Design of Structural Steel Hollow Section Connections* (Syam and Chapman, 1996), in which design models are presented for commonly used tubular connections. The moment end plate connection described in this report is not included in the AISC publication, since an appropriate design model does not currently exist. Some typical applications of the moment end plate connection using rectangular hollow sections are shown in Figure 1.

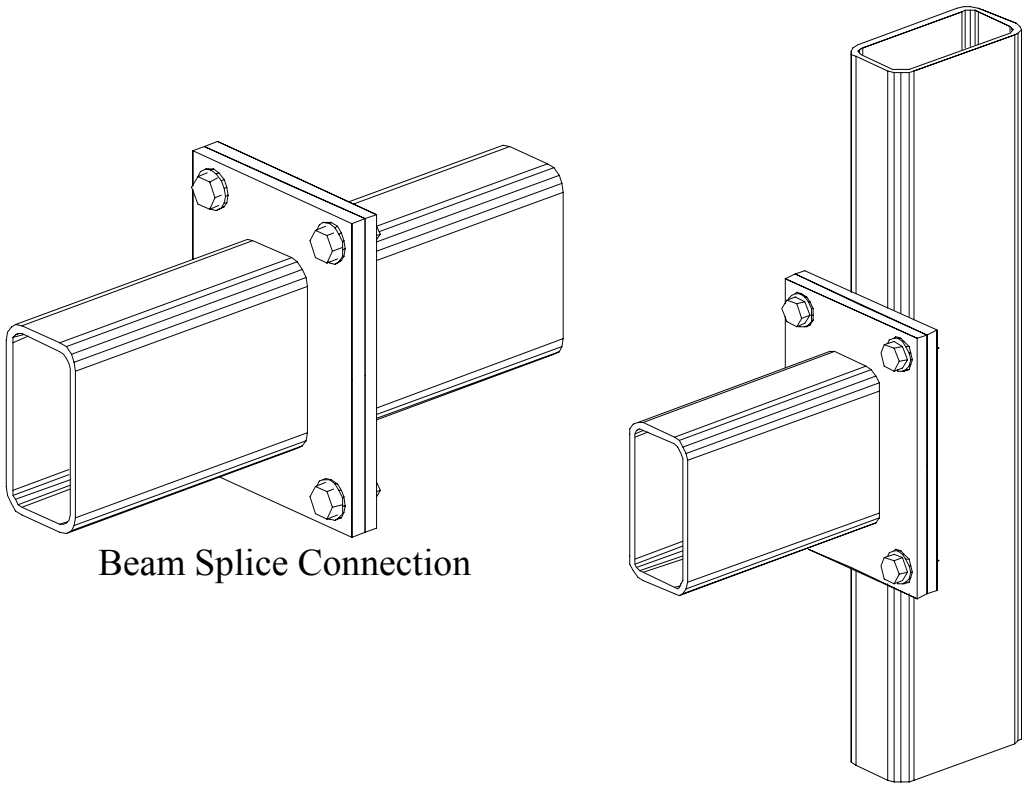

Beam Splice Connection

Beam-Column Connection

Figure 1 - Bolted Moment End Plate Connections using Rectangular Hollow Sections

The moment end plate connection joining I-section members has been used extensively, and considerable documentation on its behaviour exists in the literature (for example, Grundy *et al.,* 1980; Murray, 1988, 1990; Kukreti *et al.,* 1990). By contrast, research on end plate connections joining rectangular and square hollow sections has been limited, and furthermore has concentrated primarily upon pure tensile loading (Kato and Hirose, 1985; Packer *et al.,* 1989), or combined compression and bending (Kato and Mukai, 1991) as in a column-to-column bolted flange splice connection.

When the end plate connection is subjected to pure flexure, tensile loads are applied to those bolts on the tensile side of the neutral axis through the bending of the plate. Failure of the connection generally occurs when those bolts reach their tensile capacity. The ultimate strength of the connection may be reached either before yielding has occurred in the end plate (in which case the end plate is said to be "rigid"), or after yielding has occurred in the end plate (in which case the end plate is said to be "flexible") as outlined by Nair *et al.* (1974). While the design of rigid end plate connections may be less difficult than those with flexible end plates due to the effects of prying in the latter, the flexible end plate provides a substantially more economical and ductile connection.

The effects of prying have been studied extensively and various methods, such as the stub-tee (split tee) analogy (Agerskov, 1976; Kato and McGuire, 1973; Nair *et al.,* 1974; and Kennedy *et al.,* 1981), have been developed to predict the effect of prying on the connection strengths. These methods have primarily been associated with moment end plate connections in I-sections. While the behaviour of the end plate connection utilising rectangular hollow sections differs from that for I-sections, the stub tee analogy can be adapted to model the former connection. This is the approach followed in this report.

The behaviour of the end plate may be divided into three distinct categories based on the plate thickness and extent of loading, similar to those suggested by Kennedy *et al.* (1981). The first mode is termed *thick plate behaviour* where there are no prying effects, resulting in a direct relationship between the bolt loads and the applied moment. The third mode is termed *thin plate behaviour* where the prying force is a maximum, with the resulting bolt load being the sum of the prying forces and the forces assigned to the bolt due to the applied moment. The second mode, termed *intermediate plate behaviour*, falls between the thick and thin plate behaviour and is characterised by the prying force ranging from zero to the maximum attainable.

In this report, an analytical model to determine the moment capacity of end plate connections joining rectangular hollow sections is presented. The model is based on the modified stub-tee analogy which enables the effects of bolt prying forces to be incorporated. The model is further refined using yield line analysis to include the effect of the bolt positions along the tensile face of the end plate. The model described in this report is limited to the end plate connection containing two rows of bolts as shown in Figure 1. The predictions of the model are compared with the results obtained from the experimental program conducted at the University of Sydney (Wheeler, Clarke and Hancock, 1995a, 1995b, 1997).

2. Prying Action

The behaviour of a connection where tensile loads are transferred to fasteners through an end plate is highly dependent on the rigidity of this plate. This is demonstrated in Figure 2 where two stub tee connections are shown. In the first connection, which comprises a rigid end plate, minimal deformation occurs when the tensile load (P) is applied, with the plate remaining virtually parallel to the connecting surface. The second connection, which contains a flexible end plate, deforms as shown when loaded, generating compressive (prying) forces between the contacting surfaces which raises the tensile bolt forces correspondingly.

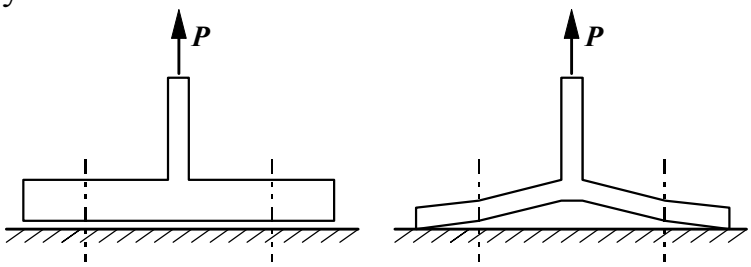

(a) Rigid End Plate (b) Flexible End Plate

Figure 2 - End Plate Behaviour

The study by Nair *et al.* (1974) into the effect of tension and prying forces found that the load capacity of bolted connections can be substantially reduced by prying action. The factors found to govern the magnitude of this prying force include the geometry and material properties of the end plate, and the size and strength of the bolts.

If it is assumed that the connection fails due to tensile fracture of the bolts, the failure load for the rigid end plate can be easily calculated by determining the tensile strength of the bolt group. For the flexible end plate, the reduced failure load (P_u) is defined as the ultimate tensile load in the bolts (B_u) minus the prying force at ultimate load (Q_u).

$$P_u = B_u - Q_u \tag{1}$$

The magnitude of the prying force (Q) depends on the flexibility of the end plate. As seen previously, Q is zero for the rigid end plate, while for the flexible end plate Q ranges from zero to Q_{max}, where Q_{max} is the maximum attainable prying force which occurs at the formation of a plastic hinge through the line of the bolts.

While the connections described in this report are not a stub tee, prying forces are considered important. By modifying the stub tee analogy, a model that effectively predicts the connection strength considering the prying forces can be developed for tubular end plate connections.

3. Experimental Study

While two types of end plate connections (termed Type A and Type B) were investigated experimentally at the University of Sydney (Wheeler, Clarke and Hancock, 1995a, 1995b, 1997), this report deals only with the Type B connection containing four bolts, as shown in Figure 3. The connections were tested in pure bending by subjecting a beam, containing a beam splice connection (Figure 1) at mid span, to a four point bending test.

The parameters varied in the experimental programme include the plate size (W_p, D_p), the plate thickness (t_p), the section shape (square or rectangular), and the position of the bolts with respect to the section flange (s_o) and the section web (c). Each test contained two rows of bolts, one above and the other below the section. The dimensions of the end plates and the type of sections used for all Type B specimens in the experimental programme are given in Table 1. The distance from the edge of the plate to the centre of the bolts (a_e) was constant for all tests and set at 30 mm according to the edge distance limits specified in the Australian Standard for Steel Structures, AS 4100 (SA, 1990). All holes were clearance holes (diameter 22mm) for M20 bolts. The end plate material was 350 grade steel, to AS 3678 (SA, 1981b) with a nominal yield stress of 350 MPa. The measured static yield stress (f_y) and ultimate tensile strength (f_u) for the end plates obtained through coupon tests are listed in Table 2.

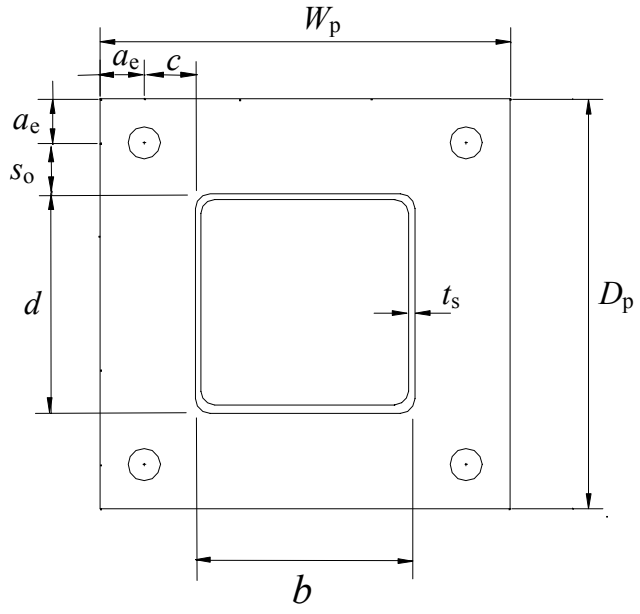

Figure 3 - End Plate Layout

To eliminate the possibility of the connection strength being limited by local buckling within the beam, all sections used were compact. The nominal section sizes are shown in Table 3, along with the measured ultimate moment capacities (M_{us}) for each type of section. The sections were manufactured to the requirements of AS 1163 (SA, 1991a), with a nominal yield stress of 350 MPa.

Table 1. End Plate Connection Details and Test Results

Specimen No.	Section Type†	Plate Dimensions (mm) t_p	W_p	D_p	s_o	c	M_{cu} (kN.m)	Failure Mode*
11	SHS	12	210	280	35	0	48.6	Deformation
12	SHS	16	210	280	35	0	69.0	Bolt
13	SHS	20	210	280	35	0	77.4	Bolt
14	RHS	12	160	330	35	0	57.1	Deformation
15	RHS	16	160	330	35	0	72.5	Bolt
16	RHS	20	160	330	35	0	86.6	Bolt
17	SHS	12	280	280	35	35	38.6	Deformation
18	SHS	16	280	280	35	35	59.5	Bolt
19	SHS	20	280	280	35	35	72.4	Bolt
20	RHS	12	230	330	35	35	48.5	Deformation
21	RHS	16	230	330	35	35	71.3	Bolt
22	RHS	20	230	330	35	35	79.6	Bolt
23	SHS	16	210	300	45	0	58.3	Bolt
24	SHS	16	210	260	25	0	66.6	Bolt
25	RHS	16	160	350	45	0	62.1	Bolt
26	RHS	16	160	310	25	0	86.0	Bolt

* *Deformation Mode: Tests terminated due to excessive end plate deformations.*
Bolt Mode: Test ultimate load dictated by bolt fracture.

† *Section dimensions are given in Table 3.*

The bolt and nut assemblies were M20 structural grade 8.8 assemblies (grade 8.8/T), manufactured to AS 1252 (SA, 1981a). The measured yield and ultimate tensile loads of the bolts were 195 kN and 230 kN, respectively. Further details on these bolt assemblies can be found in the manufacturer's catalogue (Ajax Fasteners, 1992).

Table 2 - Measured End Plate Material Properties

Plate Thickness t_p (mm)	f_y (MPa)	f_u (MPa)
12	354	499
16	349	482
20	351	496

The connections were prefabricated to AS 4100 (SA, 1990), with a combination fillet/butt weld joining the section to the end plate. This weld was SP category and qualified to AS 1554.1 (SA, 1991c), with a nominal leg length of 8 mm for the fillet.

Table 3 - Nominal Section Details

Section	Depth d (mm)	Width b (mm)	Thickness t_s (mm)	M_{us} (kN.m)
SHS	150	150	9	119
RHS	200	100	9	138

Upon assembly of the connection, the bolts were tensioned to 145 kN (60% proof stress). An incremental load was then applied to the connection by means of a stroke-controlled servo until failure occurred. As the sections were not susceptible to local buckling, the ultimate load of the specimen was limited to connection failure, which occurred either when the tensile bolts fractured, or when the longitudinal deformations of the end plate were deemed excessive. The ultimate moment (M_{cu}) and the failure mode for each test are listed in Table 1.

In most cases the ultimate failure mode for the tests was tensile bolt failure, with excessive deformations in the end plates only occurring in those specimens containing the thinner, more flexible, end plates. In all tests, the formation of yield lines was evident well before the ultimate load was reached. As each test continued, the end plate deformations increased until either excessive deformations occurred or fracture of the tensile bolts was imminent.

Changes in the end plate width (W_p) and thickness (t_p) resulted in significant changes in the ultimate load. An increase in plate thickness (t_p) increased the strength of the joint (compare SHS specimens #11, #12, and #13, and RHS specimens #14, #15 and #16). An increase in the plate width (W_p) (corresponding to moving the position of the bolts away from the line of the webs as denoted by the parameter c in Table 1) reduced the stiffness and strength of the joint (compare SHS specimens #12 and #18, and RHS specimens #15 and #21). The effect of the position of the bolts was further demonstrated through their proximity to the section flange (parameter s_o in Table 1). As the bolts were moved closer to the flange of the section, the connection stiffness and strength also increased (compare SHS specimens #23, #12 and #24, and RHS specimens #25, #15 and #26).

For the test specimens with the 12 mm end plate (specimens #11, #14, #17 and #20), the loads in the tensile bolts were well below their ultimate values when a yield line mechanism formed in the plate. This mechanism was such that the load transfer to the bolts was minimal, and fracture of the bolts would only have occurred if the test was continued until very high rotations were experienced. In practice, these tests were stopped prior to the deformations becoming excessively large.

4. Theoretical Formulation

4.1 General

Theoretical models for the bolted tubular moment end-plate connection based on yield line analysis and the stub tee analogy are presented in Sections 4.2 and 4.3, respectively. A generalised connection model for predicting the ultimate capacity of the connection involving the integration of both the yield line and stub-tee analysis is subsequently derived in Section 4.4.

The yield line analysis serves to provide an estimate of the experimental yield moment of the connection[1] (M_{cy}), which is defined by the intersection of the initial connection stiffness and the strain hardening stiffness (see Figure 4). At the connection yield moment, the end plate is assumed to contain a plastic mechanism characterised by yield lines which form when the end plate cross-section becomes fully plastic at the yield stress f_y. Prying action is not considered in the yield line analysis. As defined here, the connection yield moment may be considered to correspond to the serviceability limit state of the connection.

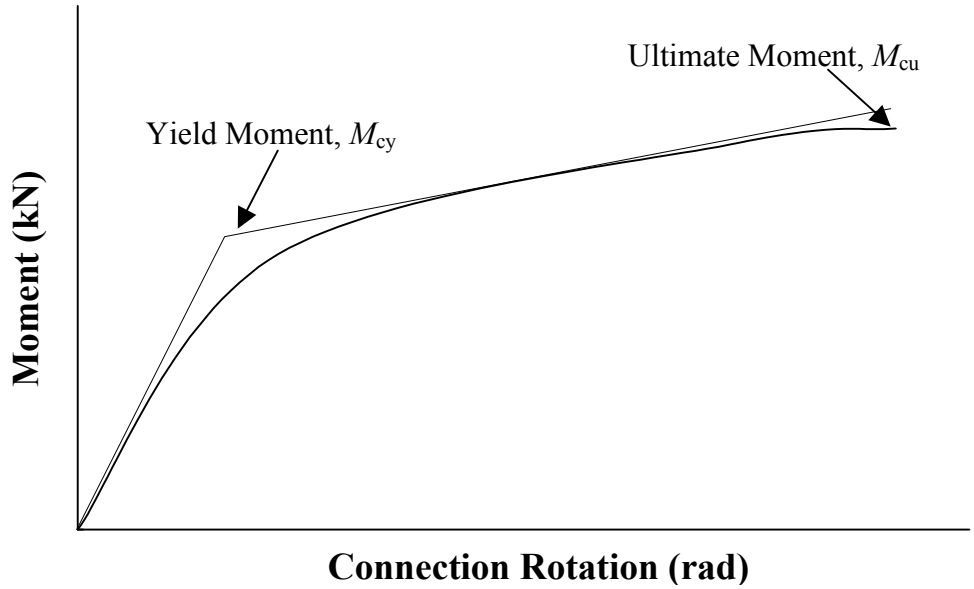

Figure 4 - Typical Connection Moment-Rotation Curve

The theoretical model based on the stub tee analogy considers the effects of prying action and aims to predict the experimental ultimate strength of the connection (M_{cu}) (see Figure 4). This model is limited by the assumption that the end plate behaves in a one-dimensional fashion due to the formation of yield lines across the width of the end plate (Modes 1 and 2 shown in Figure 5) (Agerskov, 1976; Kato & McGuire, 1973). Since the yield lines invariably

[1] The yield moment (M_{cy}) as defined here should not be confused with the moment to cause first yield of the connection.

undergo significant rotation prior to the connection ultimate strength being reached, much of the material is stressed into the strain-hardening range. For the purpose of predicting the connection ultimate moment, it is therefore appropriate to assume the yield lines are fully plastic and stressed to a level denoted f_p which is greater than the yield stress f_y but less than the ultimate tensile strength f_u.

The generalised connection model discussed in Section 4.4 constitutes a modification of the stub tee analogy to cater for the Mode 3 plastic mechanism (see Figure 5) whereby yield lines form diagonally across the tensile corners of the end plate.

4.2 Yield Line Analysis

The analysis of stub tee flange or end plate connections generally assumes that yield lines form transversely across the end plate (Agerskov, 1976; Kato and McGuire, 1973). In the present work, this assumption is valid if the bolts are positioned such that the yield lines form in this manner. In the experimental program described in Section 3, the position of the bolts was varied and other yield line mechanisms were observed.

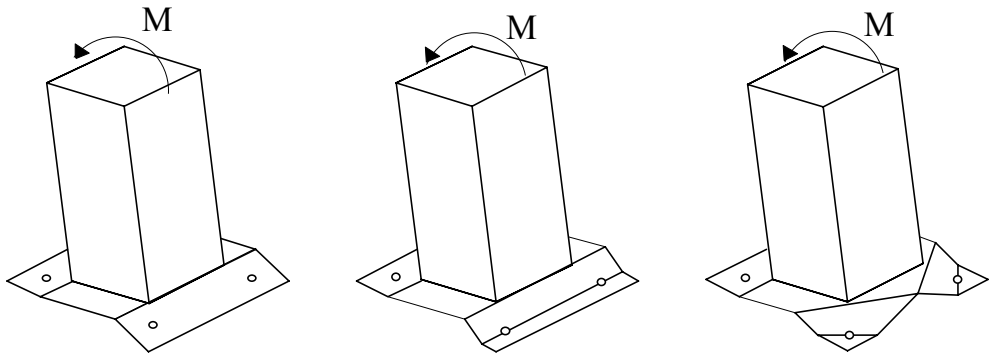

(a) Mode 1 *(b) Mode 2* *(c) Mode 3*

Figure 5 - Yield Line Modes of Failure

The three yield line mechanisms observed experimentally are shown in Figure 5. Mode 1 consists of yield lines forming at the top and bottom of the section, coupled with elongation and yielding of the tensile bolts (Figure 5a). In Mode 2, an additional yield line forms through the line of bolts on the tension side of the connection (Figure 5b). Once the Mode 2 mechanism has formed, no additional load is transferred to the tensile bolts. Mode 3 comprises a more complex arrangement of yield lines as shown in Figure 5c. As for Mode 2, the yield lines pass through the tensile bolts and no additional loads are transferred to the bolts following the yield line formation. It should be noted that in the yield line analysis presented hereafter, the effect of the end plate deformations on the work done by the tensile bolts in Mode 1 is approximated by the displacement of a constant load. Conversely, in Modes 2 and 3 the yield lines

pass through the bolt holes with no displacement of the bolts. Thus the effects of prying are not considered in the yield line analysis.

Virtual work principles are used to obtain the analytical expressions for the yield moment M_{yl} for each of the mechanisms shown in Figure 5. The variables used are defined in Figure 3, with n being the number of tensile bolts. In the yield line analysis for Mode 1, B_{yl} is taken as the yield load per bolt which was measured to be 190 kN. The position of the yield lines is assumed to be influenced by the size of the weld fillet; for this reason the depth of the section (d) and distance from the line of bolts to the section flange (s_o) are corrected to $d' = d + s/\sqrt{2}$ and $s_o' = s_o - s/\sqrt{2}$ respectively, where s is the leg length of the fillet weld. It is also assumed that the section is perfectly rectangular (neglecting the rounding of the corners).

The yield moments for Mode 1, Mode 2 and Mode 3 are respectively

Mode 1

$$M_{yl} = \left(\frac{(d' + 2 \cdot (s_o' + a_e)) \cdot w}{(s_o' + a_e) \cdot d'} \cdot m_p + \frac{n \cdot B_{yl} \cdot a_e}{s_o' + a_e} \right) \cdot (d - t_s) \qquad (2)$$

Mode 2

$$M_{yl} = \left(\frac{2 \cdot (d' + s_o') \cdot w}{s_o' \cdot d'} - \frac{n \cdot d_f}{s_o'} \right) \cdot m_p \cdot (d - t_s) \qquad (3)$$

Mode 3

$$M_{yl} = \left(\frac{w}{d'} + \frac{\frac{v \cdot w}{b} \cdot (b^2 + 4 \cdot q^2) + \left(\sqrt{r^2 + 4 \cdot v^2 \cdot q^2}\right) \cdot d_{34} + 4 \cdot u \cdot q \cdot v}{(2 \cdot q \cdot c + s_o' \cdot b) \cdot d'} \right) \cdot (d - t_s) \cdot m_p \qquad (4)$$

where
$$w = b + 2 \cdot a_e + 2 \cdot c = W_p$$
$$v = d' + s_o'$$
$$q = a_e + s_o' - u$$
$$r = 2 \cdot q \cdot c - b \cdot d'$$
$$d_{34} = \frac{a_e \cdot (2 \cdot q \cdot v - r)}{q \cdot v \cdot r} \cdot \sqrt{r^2 + 4 \cdot q^2 \cdot v^2} - 2 \cdot d_f$$

The derivation of the above expressions is given in Appendix A. For Mode 3, the yield moment M_{yl} must be minimised with respect to the variable u (see Appendix A) to obtain the correct lower bound solution.

The plastic moment per unit length (m_p) for yield line analysis is given by

$$m_p = \frac{1}{4} \cdot t_p^{\,2} \cdot f_y \tag{5}$$

where f_y is the yield stress of the end plate and t_p is the end plate thickness.

Yield line analysis by its nature results in an upper bound solution for any given mechanism. Of all possible mechanisms, the one with the lowest yield moment is taken as the governing mode. For each test specimen, the calculated yield moments for each mechanism and the governing failure mode are tabulated in Table 4. The values of yield stress f_y used in the various mechanism analyses are given in Table 2 for the end plate thickness considered.

Table 4 - Yield line Results

Test #	Experimental Yield Moment M_{cy} (kN.m)	Yield Line Moment M_{yl} Mode 1 (kN.m)	Mode 2 (kN.m)	Mode 3 (kN.m)	Yield Line Failure Mode	M_{yl}/M_{cy}	M_{yl}/M_{cu}
11	31.0	37.0	27.9	32.9	Mode 2	0.90	0.57
12	49.7	47.9	49.0	57.8	Mode 1	0.96	0.69
13	57.2	59.1	76.8	90.5	Mode 1	1.03	0.76
14	39.2	45.1	26.7	37.6	Mode 2	0.68	0.47
15	53.5	56.4	46.9	66.1	Mode 2	0.88	0.65
16	52.2	66.7	73.5	103.6	Mode 1	1.28	0.77
17	22.0	35.9	38.1	25.1	Mode 3	1.14	0.65
18	39.2	46.1	66.9	44.2	Mode 3	1.13	0.74
19	52.2	56.3	104.8	69.2	Mode 1	1.08	0.78
20	30.7	45.9	40.0	29.0	Mode 3	0.94	0.60
21	50.2	57.8	70.2	50.9	Mode 3	1.01	0.71
22	56.2	68.8	110.0	79.8	Mode 1	1.23	0.86
23	42.5	42.2	38.7	45.9	Mode 2	0.91	0.66
24	48.4	55.9	69.9	81.7	Mode 1	1.15	0.84
25	46.7	49.2	36.7	52.0	Mode 2	0.79	0.59
26	63.9	66.5	67.7	94.9	Mode 1	1.04	0.77
					Mean	1.010	0.696
					S.D.	0.159	0.106

A comparison of yield moments for Modes 2 and 3 demonstrates that sufficient spacing of the tensile bolts away from the section perimeter will cause a reduction in the connection yield moment by approximately 30 percent. The thickness (stiffness) of the end plate will also affect the mode of failure. Thicker (stiffer) end plates tend to result in failure of the bolts, while for thinner plates the failure mechanism tends to be confined to the end plate itself.

4.3 Modified Stub-Tee Method

4.3.1 General Model

The stub-tee analogy has been used in I-beam moment end plate connection models to quantitatively determine the prying forces (Kennedy *et al*., 1981; Nair *et al.,* 1974). The method involves a simple rigid plastic (yield line) analysis carried out on an analogous beam that represents the one-dimensional behaviour of the end plate with yield lines parallel to the axis of bending only. This simple representation of the connection is shown in Figure 6, with the equivalent beam having a length equal to the plate depth (D_p), and a depth equal to the plate thickness (t_p). The model assumes that the plastic hinges that form at Points 1, 2 and 3 (Figure 6) represent yield lines which form transversely across the end plate as demonstrated in Modes 1 and 2 (Figure 5). If the bolts are positioned such that a Mode 3 failure occurs, the model needs to be adjusted as discussed later in Section 4.4. Other assumptions associated with this model are consistent with those of classical beam and rigid-plastic theory.

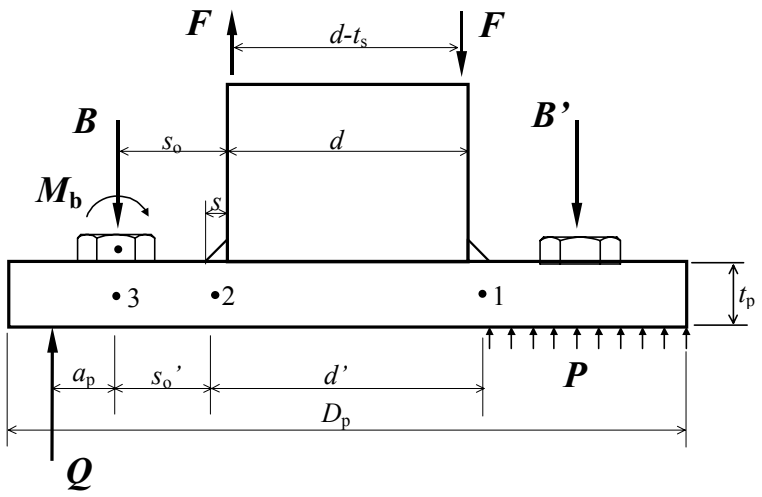

Figure 6 - Analytical Model

The moment acting on the connection (M) is assumed to be applied to the end plate through equal and opposite flange forces F acting through the centre line of the flanges, so that

$$M = F \cdot (d - t_s) \tag{6}$$

The bolt forces are assumed to act through the centre of the bolts and are denoted B and B'. The moment generated through bending of the bolts on the tensile side of the connection, resulting from the end plate deformation, is denoted M_b. The resultant of the contact forces acting on the compressive side of the end plate connection is denoted P, with the prying force on the tension side of the connection being simplified to a point load (Q) acting at a distance a_p from the line of the tensile bolts. The quantity a_p is defined as either the distance to the edge of the plate (a_e), or twice the end plate thickness ($2 \cdot t_p$), whichever is the lesser.

The tensile force (F) acting through the tensile flange of the section can be expressed in terms of the shear forces either side of the flange,

$$F = F_R + F_L \tag{7}$$

where F_L is the shear force on the left and F_R the shear force on the right side of the flange as shown in Figure 7.

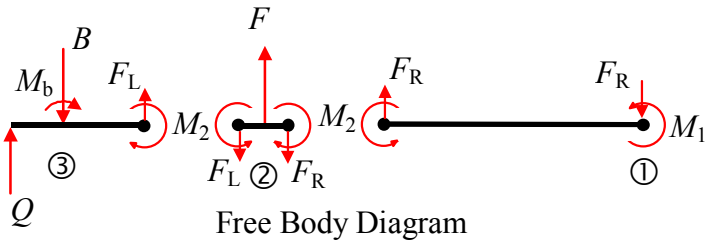

Figure 7 - Definition of Forces on Free-Body Segment of Beam

These shear forces can be expressed in terms of the bolt loads (B), the prying force (Q) and the internal moments at Points 1 and 2 (M_1, M_2) using

$$F_L = B - Q \tag{8}$$

$$F_R = \frac{M_1 + M_2}{d'} \tag{9}$$

Combining the Equations 6 - 9, the general expression for the connection moment is obtained as

$$M = F \cdot (d - t_s) = \left(B - Q + \frac{M_1 + M_2}{d'} \right) \cdot (d - t_s) \tag{10}$$

As discussed previously, the behaviour of the end plate is dependent on its thickness (t_p). Thick plate behaviour occurs when the ultimate connection failure due to bolt fracture occurs subsequent to a yield line forming at Point 1 but prior to a yield line forming at Points 2 or 3. Intermediate plate behaviour occurs when the bolts fracture after the formation of yield lines at Points 1 and 2 (Mode 1 mechanism). Thin plate behaviour corresponds to the formation of yield lines at Points 1, 2 and 3 (Mode 2 mechanism) in the end plate without deformation of the bolts.

The plastic moment M_{ip} for each of the "hinges" i shown in Figure 6 is given by

$$M_{ip} = \frac{1}{4} \cdot t_p^2 \cdot f_p \cdot l_i \tag{11}$$

where t_p is the end plate thickness, f_p is the stress along the yield line, and l_i is the length of the yield line. In the case of Points 1 and 2, the yield line length l_i is simply the width of the end plate W_p. Since the yield line at Point 3 forms

through the line of the bolts, the length of this yield line is assumed to be defined by

$$l_3 = W_p - n \cdot d_f \tag{12}$$

in which n is the number of bolts in the tensile zone and d_f is the diameter of the bolt holes.

Reflecting the influence of strain-hardening on the ultimate moment capacity of the connection, and following the approach of Packer *et al.* (1989), the stress (f_p) used to calculate the plastic moment capacity of the end plate is assumed to be intermediate in value between the yield stress (f_y) and the ultimate tensile strength (f_u) of the plate material,

$$f_p = \frac{f_y + 2 \cdot f_u}{3} \tag{13}$$

In this report, f_p is termed the plate design stress.

4.3.2 Thick Plate Behaviour

The mechanism described as thick plate behaviour is shown in Figure 8. The mechanism forms through the combination of a yield line at Point 1, and yielding of the tensile bolts. The ultimate bolt load B_u is the tensile resistance produced by n bolts, each with a tensile strength of B_{u1}.

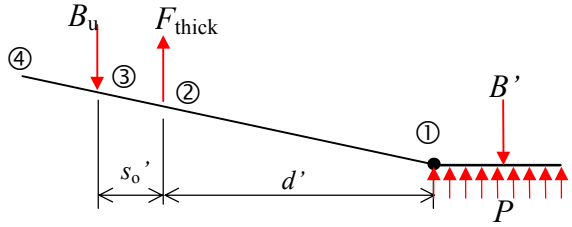

Figure 8 - Thick Plate Behaviour

For the thick plate, the prying force (Q) is zero. Also, since there is little bending in the plate away from Point 1, the resisting moment of the bolts (M_b) is neglected. The moment at Point 2 (M_2) is found by considering moment equilibrium for the left-hand segment of the beam and is expressed as

$$M_2 = B_u \cdot s_o' \tag{14}$$

From (10) and (14), setting Q and M_b to zero, and using the plastic moment at Point 1, the moment for the connection can be expressed as

$$M_{thick} = \left(\frac{M_{1p} + B_u \cdot (d' + s_o')}{d'} \right) \cdot (d - t_s) \tag{15}$$

Thick end plate behaviour is considered to hold as long as the moment at Point 2, as calculated from (14), is less that the plastic moment ($M_2 \leq M_{2p}$).

4.3.3 Intermediate Plate Behaviour

The mechanism for intermediate plate behaviour is shown in Figure 9, and is characterised by plastic hinges forming at Points 1 and 2, with the bolts on the tensile side of the connection also yielding.

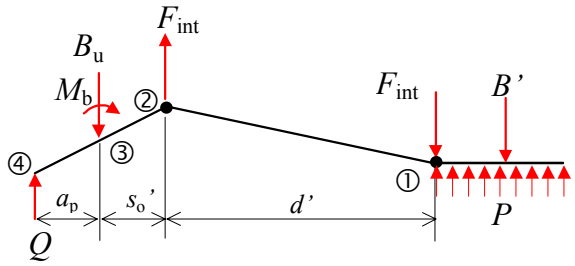

Figure 9 - Intermediate Plate Behaviour

The bolts are assumed to have attained their full plastic moment and so the resistance generated by the bending of n bolts is given by

$$M_b = n \cdot \frac{\pi \cdot d_b^3 \cdot f_{yb}}{32} \tag{16}$$

where d_b is the bolt diameter and f_{yb} is the bolt yield stress.

The free body diagram pertinent to intermediate behaviour is shown in Figure 10. As the intermediate plate behaviour commences, the prying force (Q) is zero. The prying force will attain its maximum value (Q_{max}) at the point of transition to thin plate behaviour. As previously discussed, the yield lines characteristic of intermediate plate behaviour form at Points 1 and 2, thus $M_1 = M_{1p}$ and $M_2 = M_{2p}$.

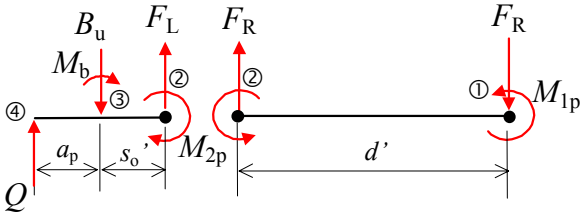

Figure 10 - Intermediate Plate Free Body Diagrams

Case 1: Prying force Q = 0

When the prying force (Q) is zero, the end plate is in the transition stage between thick and intermediate plate behaviour. At this stage, the bolt load (B) can be determined from Figure 10 by taking moments about Point 2.

$$B = \frac{M_{2p} + M_b}{s_o'} \tag{17}$$

Substituting (17) into (10), and setting the prying force to zero enables the minimum moment for the connection for intermediate behaviour to be expressed as

$$M_{\text{int}} = \left(\frac{M_{2p} \cdot (d' + s_o') + M_{1p} \cdot s_o' + M_b \cdot d'}{s_o' \cdot d'} \right) \cdot (d - t_s) \tag{18}$$

Case 2: Prying force Q > 0

When the prying force is greater than zero it can be determined through

$$Q = \frac{M_3}{a_p} = \frac{F_L \cdot s_o' - M_{2p} - M_b}{a_p} \tag{19}$$

Substituting (8) into (19) enables Q to be determined as

$$Q = \frac{B \cdot s_o' - M_{2p} - M_b}{a_p + s_o'} \tag{20}$$

Further substitution of (20) into (10) results in the expression for the moment acting on the connection during intermediate behaviour with $Q > 0$:

$$M_{\text{int}} = \left(\frac{B \cdot a_p \cdot d' + M_{2p} \cdot (d' + s_o' + a_p) + M_{1p} \cdot (a_p + s_o') + M_b \cdot d'}{(a_p + s_o') \cdot d'} \right) \cdot (d - t_s) \tag{21}$$

The above exposition on intermediate behaviour is valid from the point when the moment at Point 2, calculated from (14), exceeds the plastic moment, and while ever the moment at Point 3 is less than the plastic moment. The bolt load B must also be less than or equal to the ultimate bolt load (B_u). These conditions can be expressed in the following equations:

$$B_u \cdot s_o' \geq M_{2p} \tag{22}$$

$$F_L \cdot s_o' - M_{2p} \leq M_{3p} \tag{22}$$

4.3.4 Thin Plate Behaviour

Thin plate behaviour occurs when the moments at Points 1, 2 and 3 have reached their plastic limits (M_{1p}, M_{2p} and M_{3p}).

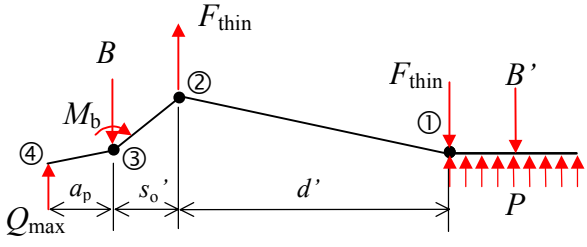

Figure 11 - Thin Plate Behaviour

Compared to intermediate plate behaviour, for thin plates an additional yield line forms at Point 3. Once this yield line forms, the prying force attains its maximum value Q_{max}:

$$Q_{max} = \frac{M_{3p}}{a_p} \tag{24}$$

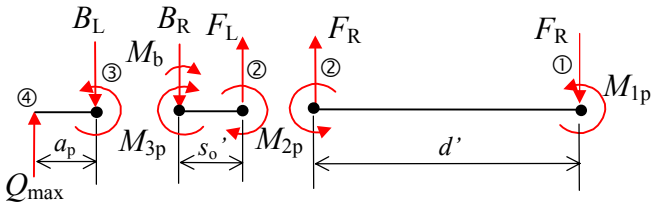

Figure 12 - Thin Plate Free Body Diagrams

The plate behaves as an intermediate plate prior to the yield line forming at Point 3. Using (20) and substituting $Q = Q_{max}$ enables the bolt load B to be expressed as

$$B = \frac{Q_{max} \cdot (a_p + s_o') + M_{2p} + M_b}{s_o'} \tag{25}$$

The resulting connection moment for thin plate behaviour is found using (24), (25) and (10), and is given by

$$M_{thin} = \left(\frac{M_{2p} \cdot (d' + s_o') + M_{3p} \cdot d' + M_{1p} \cdot s_o' + M_b \cdot d'}{d' \cdot s_o'} \right) \cdot (d - t_s) \tag{26}$$

Thin plate behaviour holds while the moment at Point 3 is equal to the plastic limit.

4.4 Generalised Connection Model

4.4.1 Ultimate Strength

While the stub tee method assumes that the yield lines form in a one-dimensional fashion across the section, the yield line analysis described in Section 4.2 demonstrated that this may not always be the case. The generalised connection model discussed in this section constitutes a modification of the stub tee analogy to cater for the Mode 3 plastic mechanism (see Figure 5) which involves inclined yield lines.

As yield line analysis is based on virtual work principles, it could be said that for a given connection with a plate of width w_p failing in Mode 3 with inclined yield lines (Figure 5c), there is an "equivalent" connection with an "equivalent" end plate width w_{eq} that fails by a Mode 2 mechanism (Figure 5b) with the one-dimensional patterns of yield lines. This equivalent width w_{eq} is determined using (3) and is expressed as

$$w_{eq} = \left(\frac{4 \cdot M_{yl}}{(d - t_s) \cdot t_p^2 \cdot f_p} + \frac{n \cdot d_f}{s_o'} \right) \cdot \frac{d' \cdot s_o'}{2 \cdot (d' + s_o')} \tag{27}$$

where M_{yl} is the yield moment corresponding to the Mode 3 mechanism.

The modified stub tee method identified two failure modes which are bolt capacity and end plate capacity. Bolt capacity (which may occur in conjunction with thick or intermediate plate behaviour) occurs when the tensile bolts fracture, while plate capacity (thin plate behaviour) occurs when a plastic mechanism forms in the end plate. The plate capacity is independent of the bolt loads.

Utilising the modified stub tee method with appropriate equivalent widths (w_{eq}), and the defined plate design stress (f_p) (Equation 13), the predicted moment for both the bolt and plate capacities for the connections outlined in Table 1 can be determined. These moments, along with the ratio of the predicted ultimate moment to the experimental ultimate moment, are given in Table 5. The predicted moments versus experimental moments are also presented in Figure 13.

Table 5 – Connection Ultimate Moments Predicted using the Modified Tee-Stub with Equivalent Width

Test #	Plate Equivalent Width w_{eq} (mm)	Predicted Moment Based on Bolt Capacity $M_{cu\text{-}th}$ (kN.m)	Predicted Moment Based on Plate Capacity $M_{cu\text{-}th}$ (kN.m)	Governing Failure Mode*	Ratio $M_{cu\text{-}th}/M_{cu}$
11	210.00	47.84	41.77	End Plate (2)	0.86
12	210.00	60.80	68.18	Bolt	0.88
13	210.00	75.37	104.41	Bolt	0.97
14	160.00	58.40	42.56	End Plate (2)	0.75
15	160.00	71.67	67.84	End Plate (2)	0.94
16	160.00	85.12	102.52	Bolt	0.98
17	191.12	46.48	38.29	End Plate (3)	0.99
18	191.12	58.57	62.09	Bolt	0.98
19	191.12	71.83	94.75	Bolt	0.99
20	172.03	59.45	45.45	End Plate (3)	0.94
21	172.03	73.39	72.89	End Plate (3)	1.02
22	172.03	87.86	110.54	Bolt	1.10
23	210.00	53.58	53.58	End Plate (2)	0.92
24	210.00	70.95	97.88	Bolt	1.07
25	160.00	62.54	52.73	End Plate (2)	0.85
26	160.00	84.50	98.58	Bolt	0.98
				Mean	0.95
				S.D.	0.088

* For connections governed by end plate capacity the relevant yield line mechanism is noted in the brackets (see Figure 5)

The statistical analysis shows a good correlation between the experimental and the predicted results. The mean and standard deviation of the predicted to test ratios for all the tests was 0.95 and 0.088 respectively. These results can be further divided into two categories depending on whether the ultimate capacity was limited by plate capacity or bolt capacity.

The connections with a tensile bolt failure mode demonstrated an excellent correlation with the test results, having a mean of 1.00 and a standard deviation of 0.066. In these connections, the deformations of the end plates were not as severe as in the thin plates, and the assumption that the end plate behaves in the same manner as a wide beam is appropriate. The connections characterised by an end plate failure mode showed a less accurate correlation with the experimental results, having a mean ratio of predicted to experimental moments of 0.91 and a standard deviation of 0.088. The low average predicted strength of the connections with a thin end plate is thought to be a result of the fact that the model does not incorporate the tension stiffening effects which occur in practice when the end plates deform significantly.

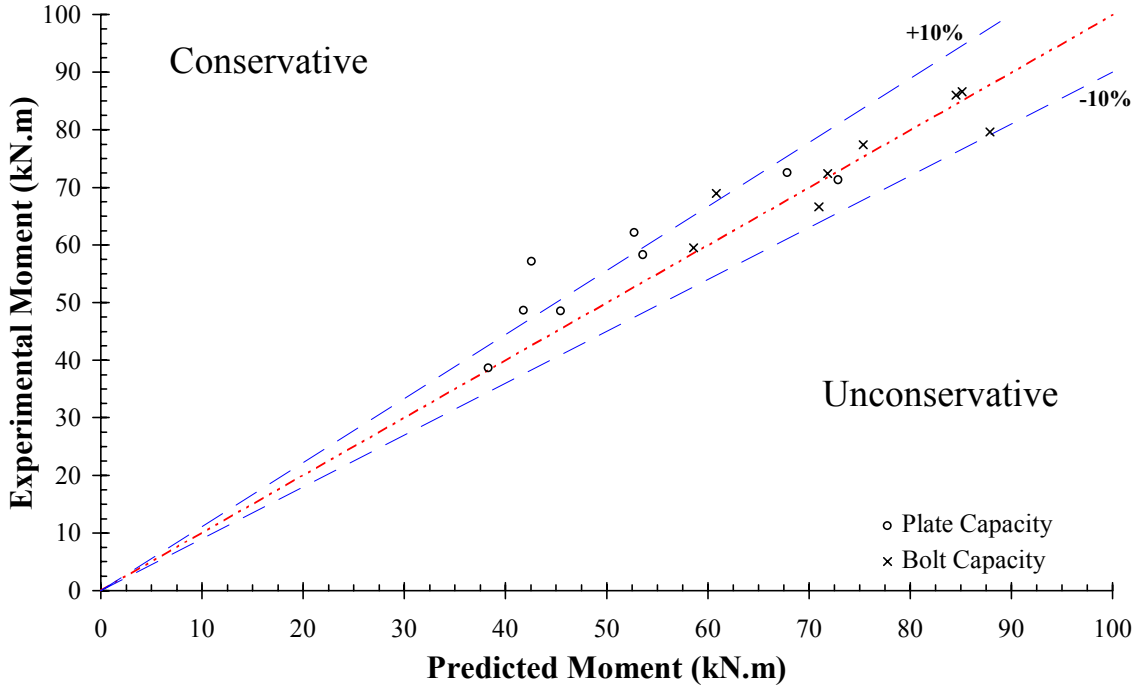

Figure 13 - Predicted versus Experimental Moment

The equivalent width is calculated assuming the section is square or rectangular (without rounded corners). Since the yield line analysis for the Mode 3 mechanism is sensitive to the position of the section corners, and since the tested sections comprised rounded corners (of external radius 2.5 times the thickness), the estimated yield moments calculated using Equation 5 are larger than results obtained by a more precise yield line analysis. As a result, for the

tests where the equivalent width concept was used (#17 to #22), the predicted to experimental moment ratios are generally higher than for the other tests.

As described in this report, the calibration of the connection model is based on tests for which the sections are relatively shallow (d = 150 or 200 mm) compared to I-sections often used in moment end plate connections. It is recognised, however, as observed by Murray (1988), that for deeper sections the yield lines through Point 1 (Figure 6) may not form due to insufficient rotations at this point. For this reason, an upper limit of 400 mm on the depth of the section has been applied to the design model described in this paper.

4.4.2 Serviceability Limits

To determine the serviceability limit moments (M_{cs}) of the connection, yield line analysis is utilised. The yield line moment capacity per unit length is assumed to be based on the plate yield stress (f_y) rather than the plate design stress (f_p), the latter being appropriate for ultimate strength calculations only. The serviceability limit is defined as when either the tensile bolts commence to yield, or the end plate forms a plastic mechanism. The moment at which the bolts begin to yield (Mode 1 yield line failure) is determined from Equation 2, while the formation of a plastic mechanism in the end plate (without bolt deformation) is described by the Mode 2 and Mode 3 mechanism analyses. The calculated serviceability limits and the relevant governing mode, which correspond precisely to the yield line analysis described in Section 4.2, are given in Table 4 (ie. $M_{cs} = M_{yl}$). The experimental yield moments (M_{cy}) and ultimate moments (M_{cu}) are given in Tables 4 and 1 respectively.

The ratios of the predicted to experimental serviceability limit moments shown in Table 4 vary depending on the plate stiffness. The thinner plates (#11, #14, #17 and #20), for which the connection rotation capacity is high, have experimental serviceability ratios (M_{cs}/M_{cu}) that are lower than those for the respective thicker plates (#13, #16, #18 and #22). Additionally, the “knee” in the moment-rotation curve (corresponding to the yield moment shown in Figure 4) for the thinner plates is accurately predicted by the serviceability limits. The plate capacity, bolt capacity and the serviceability limits are plotted on each experimental moment-rotation curve in Appendix B.

5. Design Model

The design model presented here relates to a bolted moment end plate connection connecting square or rectangular hollow sections. The connection is assumed to consist of two rows of high strength structural grade bolts (8.8/TB), which are tensioned to the minimum bolt tension as specified in AS 4100 (SA, 1990). The layout of the end plate is shown in Figure 14, with the depth of the beam section (d) assumed to be no greater than 400 mm.

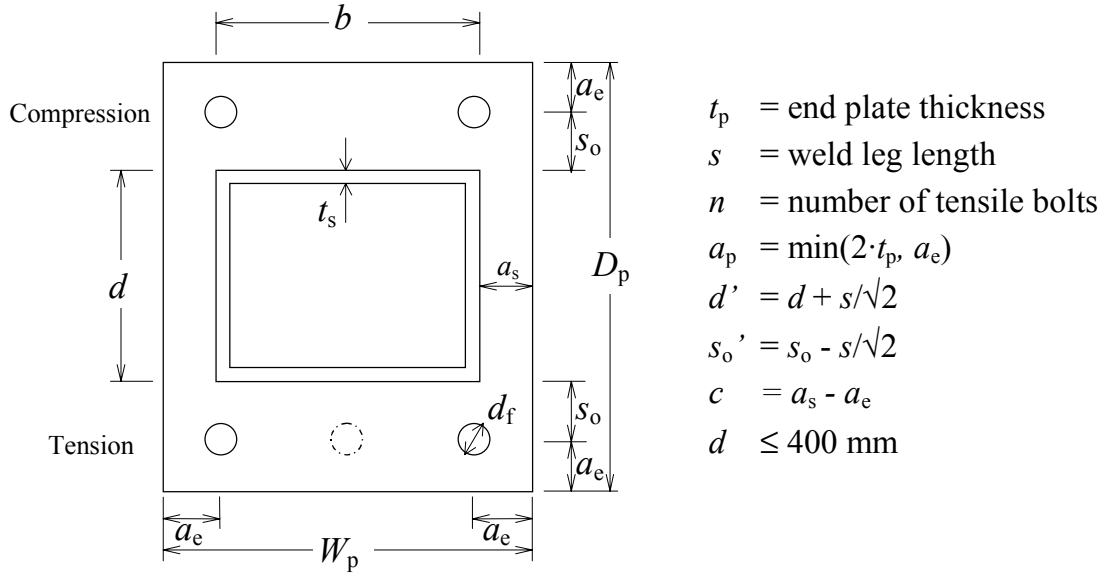

Figure 14 -Model Parameters

A major recommendation of this report is that the end plate in the bolted moment end plate connection should behave in an intermediate manner to achieve an economical and ductile design. The disadvantage of a thin end plate is that it exhibits low stiffness, causing large deformations which reduces the serviceability limit moment of the connection relative to the connection ultimate moment. On the other hand, a connection with an end plate classified as thick can fail in a brittle manner due to bolt fracture and may also be unnecessarily expensive. Thus, the report suggests that the "ideal" failure mode should involve bolt capacity combined with intermediate plate behaviour.

Following the philosophy of Murray (1990), it is assumed that the bolts in the compressive region resist all the shear loads. It is recommended that the tensile bolts be positioned so that two or more bolts fall between the line of the webs ($c=a_s-a_e \leq 0$, see Figure 14). If this condition is not met, a lower bound analysis such as the one carried out using yield line analysis (Section 4.2) will be necessary to calculate the equivalent end plate width (w_{eq}).

The strength limit state moment capacity of the connection (M_{cu}), will be the lower value of the ultimate moments computed on the basis of bolt capacity (M_{cb}) and plate capacity (M_{cp}). The connection serviceability moment (M_{cs}),

will be the minimum of the moments that cause yielding of the bolts (M_{cbs}) or yielding of the end plate (M_{cps}).

The resisting moment generated by the bolts (M_b) and the plate design stress in the end plate (f_p) are defined by Equation 16 and Equation 13, respectively. The corresponding material properties should be the nominal values obtained from the appropriate standards.

5.1 Strength Limit State Design

The moment capacity of the connection is determined using the modified stub-tee method which includes the effects of prying forces. Equations to calculate the connection capacity based on bolt failure and end plate failure are presented. The moment capacity of the connection will be the lower of these two values.

5.1.1 Connection Capacity Limited by Bolt Failure

Bolt failure is premised on intermediate plate behaviour (Section 4.3.2). The bolt load at failure is equal to the nominal tensile strength of all tensile bolts (B_u), and the stress in the end plate yield lines is equal to the plate design stress (f_p) as defined by Equation 13. The bolt load B_{u1} is the tensile strength of an individual bolt. Since it is assumed that tensile failure of the bolts govern in this case, it is appropriate that the capacity reduction factor for bolts in tension (ϕ_b) be used.

Moment Capacity

From an adaptation of Equation 21, the connection design moment capacity is given by

$$\phi_b M_{cb} = \phi_b \left(\frac{4 \cdot n \cdot \left(B_{u1} \cdot a_p + \frac{\pi \cdot d_b^3 \cdot f_{yb}}{32} \right) \cdot d' + w_{eq} \cdot \left(d' + 2 \cdot \left(s_o' + a_p \right) \right) \cdot t_p^2 \cdot f_p}{4 \cdot \left(a_p + s_o' \right) \cdot d'} \right) \cdot \left(d - t_s \right) \quad (28)$$

Design Thickness

If the connection design moment M^* is known, the appropriate end plate thickness is given by

$$t_{bu} = \sqrt{\frac{4 \cdot \left(\frac{M^* \cdot \left(a_p + s_o' \right)}{\phi_b \cdot \left(d - t_s \right)} - n \cdot \left(B_{u1} \cdot a_p + \frac{\pi \cdot d_b^3 \cdot f_{by}}{32} \right) \right) \cdot d'}{w_{eq} \cdot \left(d' + 2 \cdot \left(s_o' + a_p \right) \right) \cdot f_p}} \quad (29)$$

The limits on the plate thickness for the capacity limited by bolt failure are

$$t_p \le \sqrt{\frac{4 \cdot n \cdot B_{u1} \cdot s_o'}{w_{eq} \cdot f_p}} \tag{30}$$

5.1.2 Connection Capacity Limited by End Plate Failure

The equations for end plate capacity are based on thin plate behaviour (Section 4.3.3) using the plate design stress (f_p) (Equation 13). Since the capacity of the plate is assumed to govern in this case, with no significant contribution from the bolts, it is appropriate that the capacity factor for the plate in bending (ϕ_p) be used.

Moment Capacity

From an adaptation of Equation 26, the connection design moment capacity is given by

$$\phi_p M_{cp} = \phi_p \left(\frac{t_p^2 \cdot f_p \cdot \left(w_{eq} \cdot \left(d'+2 \cdot s_o'\right) + \left(w_{eq} - n \cdot d_f\right) \cdot d'\right) + n \cdot \frac{\pi \cdot d_b^3 \cdot f_{yb}}{8} \cdot d'}{4 \cdot d' \cdot s_o'} \right) \cdot \left(d - t_s\right) \tag{31}$$

Design Thickness

For a given connection design moment M^*, the appropriate end plate thickness is given by

$$t_{pu} = 2 \cdot \sqrt{\frac{\left(\frac{M^* \cdot s_o'}{\phi_p \cdot \left(d + t_s\right)} - n \cdot \frac{\pi \cdot d_b^3 \cdot f_{by}}{32} \right) \cdot d'}{\left(w_{eq} \cdot \left(d'+2 \cdot s_o'\right) + \left(w_{eq} - n \cdot d_f\right) \cdot d'\right) \cdot f_p}} \tag{32}$$

5.2 Serviceability Limit State Design

The serviceability moment is based on yield line analysis. Serviceability limits for the connection occur when either the bolts or the end plate begin to yield. Equations 33 and 34 following give the serviceability moments for connections whose plate parameters are known, while Equations 35 and 36 enable the appropriate plate thickness to be calculated for a given serviceability moment M_s^*. The bolt load B_{y1} corresponds to the yield load of an individual bolt.

Serviceability Moments

The serviceability limit moment based on bolt yielding ($\phi_b M_{cbs}$) is given by

$$\phi_b M_{cbs} = \phi_b \left(\frac{\left(d'+2 \cdot \left(s_o'+a_e\right)\right) \cdot w_{eq} \cdot t_p^2 \cdot f_y}{4 \cdot \left(s_o'+a_e\right) \cdot d'} + \frac{n \cdot B_{y1} \cdot a_e}{s_o'+a_e} \right) \cdot \left(d - t_s\right) \tag{33}$$

The serviceability limit moment based on plate yielding ($(\phi_p M_{cps})$ is given by

$$\phi_p M_{cps} = \phi_p \left(\frac{\left((d'+s_o')\cdot w_{eq} - n\cdot d_f \cdot d'\right)\cdot t_p^2 \cdot f_y}{2\cdot s_o'\cdot d'} \right)\cdot (d - t_s) \qquad (34)$$

Serviceability Thickness

If the connection design serviceability moment M_s^* is known, the required plate thickness to satisfy the serviceability requirements based on bolt yielding and plate yielding are given respectively by

$$t_{bs} = 2\cdot\sqrt{\frac{\frac{M_s^*\cdot(s_o'+a_e)\cdot d'}{\phi_b\cdot(d-t_s)} - n\cdot B_{y1}\cdot a_e\cdot d'}{(d'+2\cdot(s_o'+a_e))\cdot w_{eq}\cdot f_y}} \qquad (35)$$

$$t_{ps} = \sqrt{\frac{2\cdot M_s^*\cdot s_o'\cdot d'}{\phi_p\cdot(d-t_s)\cdot\left((d'+s_o')\cdot w_{eq} - n\cdot d_f\cdot d'\right)\cdot f_y}} \qquad (36)$$

5.3 Design Procedure

As discussed by Kennedy *et al.* (1981), a well designed and efficient connection is governed by the bolt capacity (Equation 28-29). Connections governed by plate capacity are generally inefficient with the serviceability limit to strength limit ratio (M_{cu}/M_{cs}) being considerably lower than those governed by bolt capacity. Connections governed by plate capacity are also more influenced by tension stiffening effects in the end plate which are not considered in the design model described in this report.

The recommended procedure for the design of the connection as described in Figure 14 is as follows:

(1) Estimate the end plate dimensions for initial design based on section size, bolt size and number of bolts.

(2) If two or more bolts are not positioned within the webs of the section ($c \le 0$), yield line analysis is required to determine the equivalent width (w_{eq}). Otherwise the equivalent width is equal to the end plate width (W_p). *(If plate thickness already determined go to (6)).*

(3) Solve for the strength limit state design thicknesses by substituting the design moment, ultimate bolt loads and plate properties into Equations 29 and 31 to obtain t_{bu} and t_{pu} respectively.

For appropriate ultimate strength limit state design, the required plate thickness is equal to the maximum of the thickness based on bolt and plate capacity (Equations 29 and 32),

$$t_u = \max(t_{bu} , t_{pu})$$

(4) Solve for the serviceability design thickness by substituting the serviceability moment, the yield load of the bolt, and the plate yield stress into Equations 34 and 36 to obtain t_{bs} and t_{ps} respectively.

For appropriate serviceability limit state design, the required plate thickness is equal to maximum of the serviceability thicknesses calculated (Equations 35 and 36).

$$t_{sv} = \max(t_{bs} , t_{ps})$$

(5) The resulting thickness for the end plate (t_p) must exceed both the serviceability and ultimate limit state thicknesses, but must be less than the maximum allowable plate thickness (t_{max}) given by Equation 30, that is

$$\max(t_{sv}, t_u) \le t_p \le t_{max}$$

(6) Solve Equations 28 and 31 using t_p to obtain the design moment capacities of the connection ($\phi_b M_{cb}$ and $\phi_p M_{cp}$). If $\phi_b M_{cb} > \phi_p M_{cp}$, either select an alternative bolting arrangement to lower the bolt capacity, or a thicker plate to increase the plate capacity. Similarly if $\phi_b M_{cb} < M^*$ the bolt capacity must be increased. Recalculate moment capacities to ensure they exceed the design moment.

(7) Solve Equations 33 and 34 to ensure that the serviceability limit moments $\phi_b M_{cbs}$ and $\phi_p M_{cps}$ are greater than the serviceability design moment M_s^*.

(8) The serviceability limit moment is the minimum moment from (7), while the connection design capacity for the strength limit state is the minimum moment from (6).

5.4 Design Examples

5.4.1 Example 1

Given the section size, end plate size, and bolts details, determine the design ultimate moment and shear capacities for the connection.

Section	125 x 75 x 4 RHS, Grade 350
End Plate	265 x 135 x 16 end plate, Grade 350
Bolts	four M16 Grade 8.8

The nominal yield stress and ultimate tensile strength for the end plate material are determined from AS 3678 (SA, 1981) as f_y = 350 MPa and f_u = 450 MPa. From Equation (13), the resulting plate design stress is f_p = 416 MPa.

The proof load, nominal tensile strength and yield load of the bolts are determined from the Ajax Fasteners handbook (1992) as B_p = 91.0 kN, B_{u1} = 125 kN and B_{y1} = 100 kN respectively, with the bolts positioned 30 mm from the edge of the end plate. From AS 4100 (1990), the capacity factors are ϕ_b = 0.8 for the bolt failure and ϕ_p = 0.9 for plate failure in plastic bending.

The weld leg length is specified to be 4 mm, giving d' = 127.8 mm and s_o' = 37.2 mm.

1. The plate dimensions and section sizes are given.

2. The bolts are in line with the web so $w_{eq} = W_p$.

   Thickness of the end plate is known, therefore go to (6).

6. Solve to obtain design capacities (Equations 28 and 31)
   $\phi_b M_{cb}$ = 22.2 kN.m and $\phi_p M_{cp}$ = 25.9 kN.m

7. Solve to obtain serviceability limits (Equation 34 and 35)
   $\phi_b M_{cbs}$ = 17.6 kN.m and $\phi_p M_{cps}$ = 18.1 kN.m

8. For the connection described, the serviceability limit moment is 17.6 kN.m, and the design ultimate moment capacity is 22.2 kN.m

For the 125 × 75 × 4 RHS, the design section plastic moment capacity (ϕM_s) is 19.0 kN.m (AS 4100), thus for the connection described, the ultimate strength is governed by the section capacity rather than the connection capacity.

The shear capacity of the connection is also determined by assuming that all shear is taken by the compressive bolts, resulting in a design shear capacity of 118.6 kN to AS 4100 (1990).

5.4.2 Example 2

The section size and the design moment are given; design the connection plate thickness and number of bolts.

Section size 150 x 150 x 6 SHS, Grade 350
Design moment (M^*) of 35 kN.m
Serviceability limit (M_s^*) of 21.5 kN.m

Assume 350 Grade end plate, the distance from the edge to centre of bolt holes is 30 mm, the distance to the flange of the section is 40 mm, and that the bolts are in line with the webs of the section. The weld leg length is 6 mm. From AS4100, the capacity factors are $\phi_b = 0.8$ for the bolts and $\phi_p = 0.9$ for the plate.

1. Assume four M16 Grade 8.8 bolts, plate width of 210 mm and depth of 290 mm. Bolt properties are tensile strength of 125 kN and yield load of 100 kN.

2. The bolts are positioned in line with the webs so $w_{eq} = W_p$.

3. Substituting into Equations 29 and 32 gives
   $t_{bu} = 17.2$ mm and $t_{pu} = 13.5$ mm. Thus $t_u = 17.2$ mm.

4. Substituting into Equations 35 and 36 gives
   $t_{bs} = 13.6$ mm and $t_{ps} = 12.3$ mm. Thus $t_s = 13.6$ mm.

5. The maximum allowable end plate thickness (t_{max}) is 20.2 mm.
   The required end plate thickness must be in the range
   $$\max(t_s, t_u) \le t_p \le t_{max}$$
   ie. $17.2 \le t_p \le 20.2$ Therefore, assume $t_p = 18$ mm.

6. The design ultimate strength limit state moment capacities are
   $\phi_b M_{cb} = 37.0$ kN.m and $\phi_p M_{cp} = 60.7$ kN.m.
   Since $M^* < \phi_b M_{cb} < \phi_p M_{cp}$, the strength limit state is OK.

7. The serviceability limit state moments are
   $\phi_b M_{cbs} = 29.8$ kN.m and $\phi_p M_{cps} = 45.8$ kN.m
   Since $M_s^* < \phi_b M_{cbs}$, the serviceability limit state is OK.

8. The strength limit state design moment capacity for the connection is 37.0 kN.m, and the serviceability limit state moment is 29.8 kN.m.

The connection requires an 18 mm end plate with four M16 Grade 8.8 bolts.

5.4.3 Example 3

Suppose it is required that the design moment capacity of the end plate connection exceed the design section moment capacity, for the end plate given below. Find the end plate thickness and the maximum design serviceability moment.

End Plate	330 x 230 Grade 350
Section	200 x 100 x 4 RHS
	(design section capacity to AS4100 is 51.5 kN.m.)

It is assumed that the distance from the edge of the plate to the centre of the bolts is 30 mm, the weld leg length is 4 mm, and 4 M24 bolts are used. The bolts have a yield load of 233 kN and an ultimate load of 293 kN.

1. Plate dimensions already specified.

2. The bolts are positioned outside the line of the webs; using yield line analysis an equivalent width (w_{eq}) of 177.3 mm is determined.

3. Substitution into Equations 30 and 32 gives
   t_{bu} = 5.9 mm and t_{pu} = 14.3 mm, thus t_u = 14.3 mm.

4. Serviceability limit thickness not required.

5. Select t_p =15 mm.

6. With a plate thickness (t_p) of 15 mm, the limit state moments are
   $\phi_b M_{cb}$ = 65.8 kN.m and $\phi_p M_{cp}$ = 56.0 kN.m.
   Since $\phi_b M_{cb} > \phi_p M_{cp}$, try 15 mm end plate with three tensile M16 bolts (five bolts in total). This bolting arrangement results in a Mode 2 yield mechanism, thus w_{eq} = 230 mm.
   Hence $\phi_b M_{cb}$ = 52.3 kN.m and $\phi_p M_{cp}$ = 65.8 kN.m.
   Now $\phi_b M_{cb} < \phi_p M_{cp}$ and the limit state strength is OK.

7. Assuming the end plate thickness is 15 mm with five M16 Grade 8.8 bolts gives serviceability limit moments of
   $\phi_b M_{cbs}$ = 41.1 kN.m and $\phi_p M_{cps}$ = 45.9 kN.m.

8. The strength limit state design moment capacity for the connection is 52.3 kN.m, and the serviceability limit moment is 41.1 kN.m.

The required end plate has a thickness of 15 mm and contains five M16 bolts.

6. Conclusions

This report presents a simple and accurate model to predict the strength of a moment end plate connection in rectangular hollow sections. The model uses a modified stub tee analogy, coupled with yield line analysis, to predict both the ultimate moment capacity and maximum serviceability moment for the connection. The modified stub tee incorporates the effects of the prying forces on the connection strength, while the yield line analysis predicts the failure mechanism of the end plate to enable the calculation of an end plate "equivalent width" to be used in conjunction with the stub tee model.

The model is limited to square and rectangular sections with two rows of bolts, one row above the top flange and one row below the bottom flange. While the connections tested experimentally and used for model verification only contained two bolts in each row, the addition of extra bolts in the tensile bolt row will not invalidate the model. The reason for this is that the use of additional bolts in the tensile row will tend to enforce a Mode 2 end plate failure, for which the model presented in this paper is well suited.

Of the three types of plate behaviour presented (thick, thin and intermediate), it is recommended that the end plate connections should be designed to behave according to the intermediate plate model, with connection strength being governed by bolt failure. Thin plate behaviour results in connections that are very ductile and exhibit extremely high rotations, while connections exhibiting thick plate behaviour are very brittle. The serviceability limit presented is based on first yield of the bolts or the formation of a yield mechanism in the end plate.

Comparisons of the predicted connection ultimate moments were made with the corresponding experimental results. The model demonstrated a good correlation with the test results, with an overall mean predicted to experimental ratio of 0.95, and a corresponding standard deviation of 0.088 for the range of connections tested. The model is effective in its consideration of all relevant failure modes which can occur, including bolt fracture and plastic mechanism formation in the end plate.

7. References

Agerskov, H., (1976), "High-Strength Bolted Connections Subject to Prying," *Journal of Structural Division*, ASCE, **102**(1), 161-175.

Ajax Fasteners (1992), *Fasteners Handbook - Bolt Products*, Richmond, Victoria, Australia.

Grundy, P., Thomas, I. R. and Bennetts, I. D., (1980). "Beam-to-Column Moment Connections," *Journal of Structural Engineering*, ASCE, **106**(1), 313-330.

Kato, B. and Hirose, R. (1985), "Bolted Tension Flanges Joining Square Hollow Section Members," *Journal of Structural Engineering*, ASCE, **111**(5), 163-177.

Kato, B. and McGuire, W. (1973), "Analysis of T-Stub Flange-to-Column Connections," *Journal of Structural Division*, ASCE, **99**(5), 865-888.

Kato, B. and Mukai, A. (1991), "High Strength Bolted Flanges Joints of SHS Stainless Steel Columns," *proceedings*, International Conference on Steel and Aluminium Structures, Singapore, May 1991.

Kennedy, N. A., Vinnakota, S. and Sherbourne A. N., (1981) "The Split-Tee Analogy in Bolted Splices and Beam-Column Connections," *Joints in Structural Steelwork*, John Wiley &sons, London-Toronto, 1981, pp. 2.138-2.157.

Kukreti, A. R., Ghassemieh, M. and Murray T. M., (1990), "Behaviour and Design of Large-Capacity Moment End Plates," *Journal of Structural Engineering*, ASCE, **116**(3), 809-828.

Murray, T. M. (1988), "Recent Developments for the Design of Moment End-Plate Connections," *Journal of Constructional Steel Research*, (10), pp 133-162.

Murray, T. M., (1990), "Design Guide for Extended End Plate Moment Connections," Steel Design Guide 4, American Institute of Steel Construction.

Nair, R. S., Birkemoe, P. C. and Munse, W. H., (1974), "High Strength Bolts Subject to Tension and Prying," *Journal of the Structural Division*, ASCE, **100**(2), 351-372.

Packer, J. A., Bruno, L., Birkemoe, P. C. (1989), "Limit Analysis of Bolted RHS Flange Plate Joints," *Journal of Structural Engineering*, ASCE, **115**(9), 2226-2241.

SA (1981a), *AS 1252-1981: High-strength Steel Structural Bolts with Associated Nuts and Washers for Structural Engineering*, Standards Australia, Sydney.

SA (1981b), *AS 3678-1981: Structural Steel - Hot-rolled plates, floorplates and slabs*, Standards Australia, Sydney.

SA (1990), *AS 4100-1990: Steel Structures*, Standards Australia, Sydney.

SA (1991a), *AS 1163-1981: Structural Steel Hollow Sections*, Standards Australia, Sydney.

SA (1991c). *AS 1554.1-1991: Structural Steel Welding - Part 1: Welding of Steel Structures*. Standards Australia, Sydney.

Syam, A. A. and Chapman, B. G., (1996), "Design of Structural Steel Hollow Sections," Australian Institute of Steel Construction, Sydney.

Wheeler A. T., Clarke M. J, and Hancock G. J., (1995a), "Tests of Bolted Flange Plate Connections Joining Square and Rectangular Hollow Sections," *Proceedings,* Fourth Pacific Structural Steel Conference, Singapore, Pergamon, 1995, Vol 2 pp 97-104.

Wheeler A. T., Clarke M. J, and Hancock G. J., (1995b), "Tests of bolted Moment End Plate Connections in Tubular Members," *Proceedings,* Fourteenth Australasian Conference on the Mechanics of Structures and Materials, Hobart, Tasmania, University of Tasmania, pp 331-336.

Wheeler A. T., Clarke M. J, and Hancock G. J., (1997), "Bending Tests of Bolted End Plate Connections in Cold Formed Rectangular Hollow Sections," *Research Report,* No. R736, Department of Civil Engineering, University of Sydney.

8. Notation

ϕ_b	capacity reduction factor for bolts in tension (= 0.8)
ϕ_p	capacity reduction factor for plates in bending (= 0.9)
a_e	distance from centre of bolt to edge of plate
a_p	lever arm for prying action
a_s	distance from section web to edge of plate
B	total load generated by tensile bolts
b	width of SHS or RHS
B_1	individual bolt load
B_u	ultimate tensile load in all tensile bolts
B_{u1}	measured tensile strength of individual bolt
B_{y1}	yield load of individual bolt
c	distance from line of section webs to centre of bolt hole
d	depth of SHS or RHS
d'	corrected section depth
d_b	diameter of bolt
d_f	bolt hole diameter
D_p	depth of end plate
F	force in flange of section
F_L	left hand component of tensile flange force
f_p	plate design stress used in connection design
F_R	right hand component of tensile flange force
f_u	tensile strength
f_y	yield stress
f_{yb}	bolt yield stress
M	moment applied to connection
M^*	connection design moment
M^*_s	connection serviceability design moment
M_b	plastic moment resistance provided by all tensile bolts
M_c	connection nominal moment capacity
M_{cb}	connection nominal moment capacity due to bolt failure
M_{cbs}	connection serviceability moment due to bolt yielding
M_{cp}	connection nominal moment capacity due to end plate failure
M_{cps}	connection serviceability moment due to end plate failure
M_{cs}	connection serviceability limit moment of connection
M_{cu}	measured ultimate connection moment
M_{cy}	measured connection yield moment
M_i	the moment at point *i* in the stub-tee model
M_{int}	calculated moment for intermediate plate behaviour
M_{ip}	end plate plastic moment at the point *i* in the stub-tee model
m_p	plastic moment of end plate per unit length
M_{pred}	predicted connection moment
M_{thick}	thick plate behaviour upper limit

M_{thin}	thin plate behaviour lower limit
M_{us}	ultimate moment capacity of the section
M_{yl}	connection yield moment based on yield line analysis
n	number of tensile bolts
P	load applied to tee stub
P_u	failure load of tee stub
Q	prying force
Q_{max}	maximum prying force
s	weld leg length
s_o	distance from section flange to centre of bolt hole
s_o'	corrected distance from section flange to centre of bolt hole
t_{bs}	end plate thickness required for serviceability based on bolt yielding
t_{bu}	end plate thickness required to prevent bolt failure
t_p	end plate thickness
t_{ps}	end plate thickness required for serviceability based on end plate yield line mechanism
t_{pu}	end plate thickness required to prevent end plate failure
t_s	thickness of section
t_{sv}	required end plate thickness for serviceability
t_u	required end plate thickness for ultimate strength
w_{eq}	equivalent end plate width
W_p	width of end plate

APPENDIX A - DERIVATION OF PLASTIC MECHANISMS

YIELD LINE MECHANISM 1

Mechanism 1 consists of two yield lines forming across the width of the end plate as show in Figure A1. The bolts at the bottom of the section are displaced as shown.

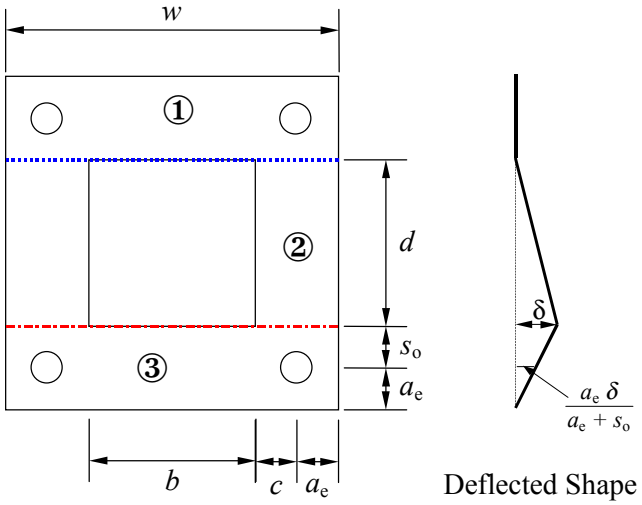

Figure A1 - Mechanism 1

The connection moment for plastic collapse of the end plate is found using virtual work principles, by prescribing a virtual displacement (δ) at the bottom of the section. Planes 1 to 3 can now be expressed in terms of their respective normal vectors.

$$n_1 = 0\mathbf{i} + 0\mathbf{j} + \mathbf{k}$$
$$n_2 = 0\mathbf{i} + \delta\,\mathbf{j} + d\,\mathbf{k}$$
$$n_3 = 0\mathbf{i} + \delta\,\mathbf{j} + (s_o + a_e)\,\mathbf{k}$$

The angle θ_{uv} between two planes, u and v defined by the normal vectors n_u and n_v is defined by:

$$\tan\theta_{uv} = \frac{|n_u \times n_v|}{|n_u \bullet n_v|} \qquad \text{(A1)}$$

which for small angles θ_{uv}, as is appropriate in virtual work calculations, can be simplified to

$$\theta_{uv} = \frac{|n_u \times n_v|}{|n_u \bullet n_v|} \qquad \text{(A2)}$$

Using Equation A2, angles θ_{uv} between intersecting planes u and v along the yield lines can be expressed as:

$$\theta_{12} = \frac{\delta}{d}$$

$$\theta_{23} = \frac{\delta \cdot (d + s_o + a_e)}{d \cdot (s_o + a_e)}$$

The lengths of the yield lines are

$$\ell_{12} = w, \quad \ell_{23} = w$$

The internal work (w_I) performed during plastic collapse can be expressed

$$w_{\mathbf{I}} = \sum_{\substack{\text{yield} \\ \text{lines}}} \ell_{\mathbf{uv}} \cdot \theta_{\mathbf{uv}} \cdot m_{\mathbf{p}} + \sum_{\text{bolts}} b_{\mathbf{y}i} \cdot \delta_i \qquad \text{(A3)}$$

In which ℓ_{uv} and θ_{uv} are as defined previously, m_p is the full plastic moment of the end plate per unit length, B_{yi} is the yield strength of the bolt i and δ_i is the elongation of bolt i. The internal work for this mechanism is therefore

$$w_I = \left(\frac{(d + 2 \cdot s_o + 2 \cdot a_e)}{(s_o + a_e) \cdot d} \cdot w \cdot \delta \cdot m_p + \frac{n \cdot B \cdot a_e}{s_o + a_e} \cdot \delta \right)$$

The corresponding external work is

$$w_E = M_{yl} \cdot \frac{\delta}{d - t_s}$$

in which M_{yl} is the applied connection moment to cause plastic collapse

Equating the internal and external work furnishes

$$M_{yl} = \left(\frac{(d + 2 \cdot s_o + 2 \cdot a_e)}{(s_o + a_e) \cdot d} \cdot w \cdot m_p + \frac{n \cdot B \cdot a_e}{s_o + a_e} \right) \cdot (d - t_s)$$

YIELD LINE MECHANISM 2

This mechanism consists of three yield lines forming across the width of the end plate as show in Figure A2. The number of bolts (n) in the row along the bottom of the section may be varied.

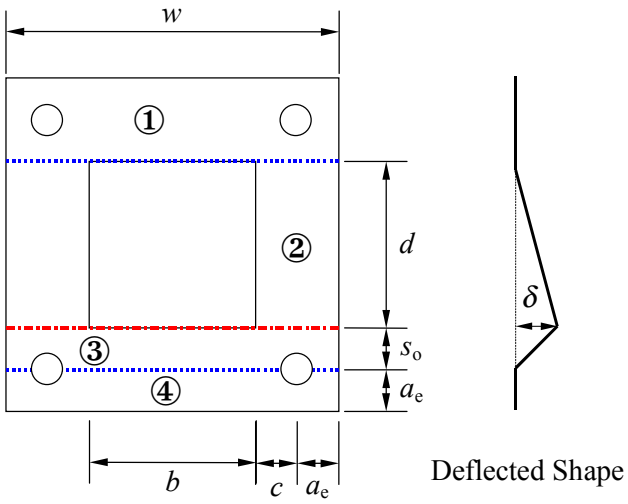

Figure A2 - Mechanism 2

The connection moment for the plastic collapse of the end plate is found using virtual work principles, by placing a virtual displacement (δ) at the bottom of the section. Planes 1 to 4 can now be expressed in terms of their respective normal vectors.

$$n_1 = 0\mathbf{i} + 0\mathbf{j} + \mathbf{k}$$
$$n_2 = 0\mathbf{i} + \delta\,\mathbf{j} + d\mathbf{k}$$
$$n_3 = 0\mathbf{i} + \delta\,\mathbf{j} + s_o\mathbf{k}$$
$$n_4 = 0\mathbf{i} + 0\mathbf{j} + \mathbf{k}$$

Using Equation A2, the angles between intersecting planes along the yield lines are:

$$\theta_{12} = \frac{\delta}{d}$$

$$\theta_{23} = \frac{\delta \cdot (d + s_o)}{d \cdot s_o}$$

$$\theta_{34} = \frac{\delta}{s_o}$$

The length of the yield lines are defined by

$$\ell_{12} = w, \quad \ell_{23} = w, \quad \ell_{34} = w - n \cdot d_{\mathrm{f}}, \quad \text{where } n = \text{no. of bolts}$$

The resulting internal virtual work can be expressed as

$$w_{\mathrm{I}} = \left(\frac{(d + 2 \cdot s_{\mathrm{o}})}{s_{\mathrm{o}} \cdot d} \cdot w + \frac{w - \mathrm{n} \cdot \mathrm{d_f}}{s_{\mathrm{o}}} \right) \cdot \delta \cdot m_{\mathrm{p}}$$

The corresponding external work is:

$$w_{\mathrm{E}} = M_{\mathrm{yl}} \cdot \frac{\delta}{d - t_{\mathrm{s}}}$$

Equating the internal and external work yields the following expression for the applied connection moment to cause the plastic collapse according to Mechanism 2:

$$M_{\mathrm{yl}} = (d - t_{\mathrm{s}}) \cdot \left(\frac{2 \cdot (d + s_{\mathrm{o}}) \cdot w}{s_{\mathrm{o}} \cdot d} - \frac{\mathrm{n} \cdot \mathrm{d_f}}{s_{\mathrm{o}}} \right) \cdot m_{\mathrm{p}}$$

YIELD LINE MECHANISM 3

The mechanism shown in Figure A3 consists of six yield lines. The yield line 12 formed by the intersection of Planes 1 and 2 lies adjacent to the top of the section across the width of the flange plate. The diagonal yield lines 23 and 25, comprising the intersection of planes 2 and 3, and planes 2 and 5 respectively, pass through the lower corners of the section and intersect the vertical axis of symmetry of the connection a distance u from the lower plate edge. Two additional yield lines pass diagonally through the tensile bolts as shown in Figure A3. A final yield line of length u extending from the lower edge of the plate lies along the vertical axis of symmetry of the connection. The bolts are assumed to remain in position with no yielding.

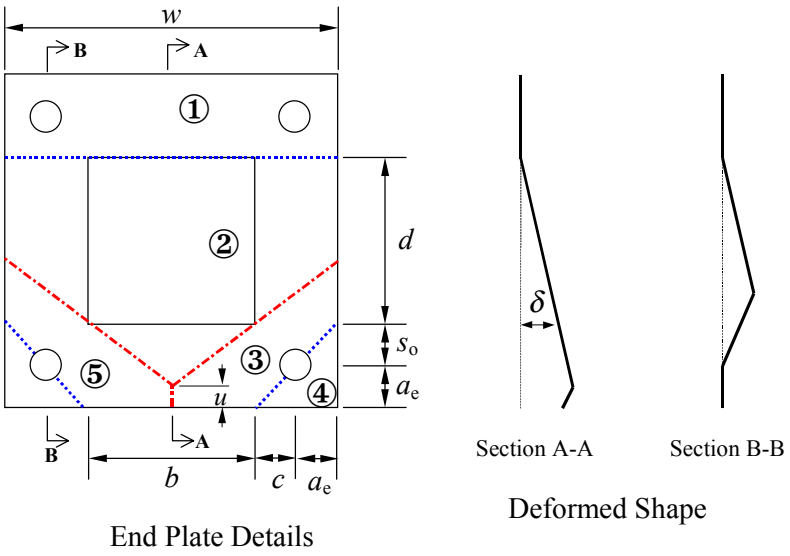

Figure A3 - Mechanism Three

The moment to cause plastic collapse of the end plate is found using virtual work principles, by placing a virtual displacement (δ) at the bottom of the section. The planes 1 through to 5 are now be expressed in terms of their normal vectors as

$$n_1 = 0\mathbf{i} + 0\mathbf{j} + \mathbf{k}$$

$$n_2 = 0\mathbf{i} + \delta\,\mathbf{j} + d\mathbf{k}$$

$$n_3 = \delta \cdot v\mathbf{i} + (2 \cdot q \cdot c - b \cdot d) \cdot \delta\,\mathbf{j} + (2 \cdot q \cdot c + s_o \cdot b) \cdot d\mathbf{k}$$

$$n_4 = 0\mathbf{i} + 0\mathbf{j} + \mathbf{k}$$

$$n_5 = -\delta \cdot v\mathbf{i} + (2 \cdot q \cdot c - b \cdot d) \cdot \delta\,\mathbf{j} + (2 \cdot q \cdot c + s_o \cdot b) \cdot d\mathbf{k}$$

where $\quad v = s_o + d$

$$q = a_e + s_o - u$$

Using Equation A2, the angles between intersecting planes along the yield lines are expressed as:

$$\theta_{12} = \frac{\delta}{d}$$

$$\theta_{23} = \frac{v \cdot \sqrt{b^2 + 4 \cdot q^2}}{(2 \cdot c \cdot q + s_o \cdot b) \cdot d} \cdot \delta$$

$$\theta_{34} = \frac{\sqrt{r^2 + 4 \cdot v^2 q^2}}{d \cdot (2 \cdot c \cdot q + s_o \cdot b)} \cdot \delta$$

$$\theta_{35} = 4 \frac{v \cdot q}{d \cdot (2 \cdot c \cdot q + s_o \cdot b)} \cdot \delta$$

The lengths of the yield lines are defined as

$$\ell_{12} = w,$$

$$\ell_{23} = \frac{w \cdot \sqrt{b^2 + 4q^2}}{2 \cdot b},$$

$$\ell_{34} = \frac{1}{2} a_e \cdot (2 \cdot v \cdot q - r) \sqrt{\left(\frac{2}{r}\right)^2 + \left(\frac{1}{q \cdot v}\right)^2} - d_f,$$

$$\ell_{35} = u$$

where $w = b + 2 \cdot a_e + 2 \cdot c = W_p$

$v = d + s_o$

$q = a_e + s_o - u$

$r = 2 \cdot q \cdot c - b \cdot d$

The contributions of each yield line to the total internal virtual work are.

$$w_{I12} = \frac{w}{d} \cdot \delta \cdot m_p$$

$$w_{I23} = \frac{v \cdot \left(b^2 + 4 \cdot q^2\right) \cdot w}{2 \cdot b \cdot \left(2 \cdot c \cdot q + s_o \cdot b\right) \cdot d} \cdot \delta \cdot m_p$$

$$w_{I34} = \theta_{34} \cdot \ell_{34} \cdot m_P$$

$$w_{I35} = 4 \frac{v \cdot q \cdot u}{\left(2 \cdot c \cdot q + s_o \cdot b\right) \cdot d} \cdot \delta \cdot m_p$$

The corresponding external work is

$$w_E = M_{yl} \cdot \frac{\delta}{d - t_s}$$

The resulting expression for the connection moment to cause plastic collapse of the end plate according to Mechanism 3 is

$$M = \left(w_{I12} + 2 \cdot \left(w_{I23} + w_{I34}\right) + w_{I35}\right) \cdot \frac{d - t_s}{\delta}$$

The expression must be minimised with respect to u to give the lower bound moment for the mechanism. By physical considerations the value for u must be greater than or equal to zero, and less than (s_o + a_e).

APPENDIX B - EXPERIMENTAL MOMENT-ROTATION CURVES

The moment-rotation behaviour of the connections tested experimentally and described in Wheeler, Clarke and Hancock (1997) are presented in this appendix. Additional data presented includes:

- The determination of the connection yield moment (M_{cy}), defined as the intersection of the initial stiffness and the strain hardening stiffness (Section 4.1).

- The computed ultimate moment capacity of the connection, as governed by bolt capacity, determined by substituting the measured material properties into Equation 21 (termed "Bolt Capacity" in the figures).

- The computed ultimate moment capacity of the connection, as governed by the formation of a plastic mechanism in the end plate, determined by substituting the measured material properties into Equation 26 (termed "Plate Capacity" in the figures).

- The yield moment of the connection, as governed by bolt yielding, determined by substituting the measured material properties into Equation 2 (termed "Bolt Yield" in the figures).

- The yield moment of the connection, as governed by yielding of the end plate, determined by substituting the measured material properties into Equation 3 or 4, whichever results in the lower value (termed "Plate Yield" in the figures).

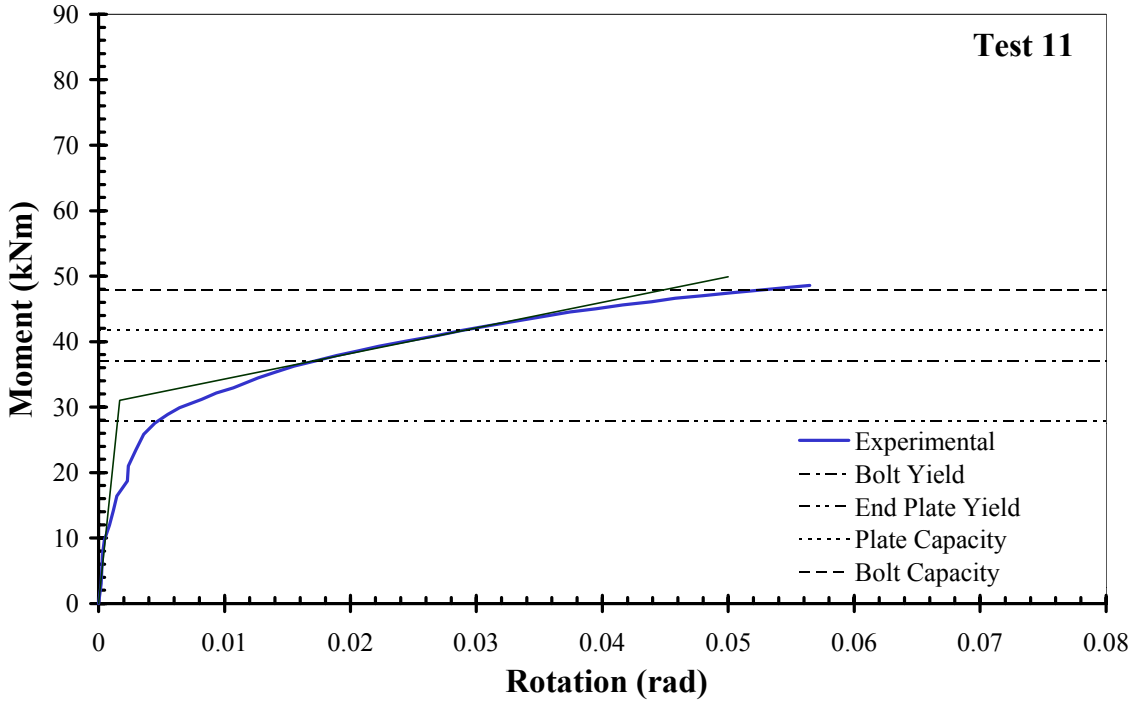

FIGURE B1 – Moment-rotation curve for Test 11
(SHS, W_p = 210 mm, t_p = 12 mm)

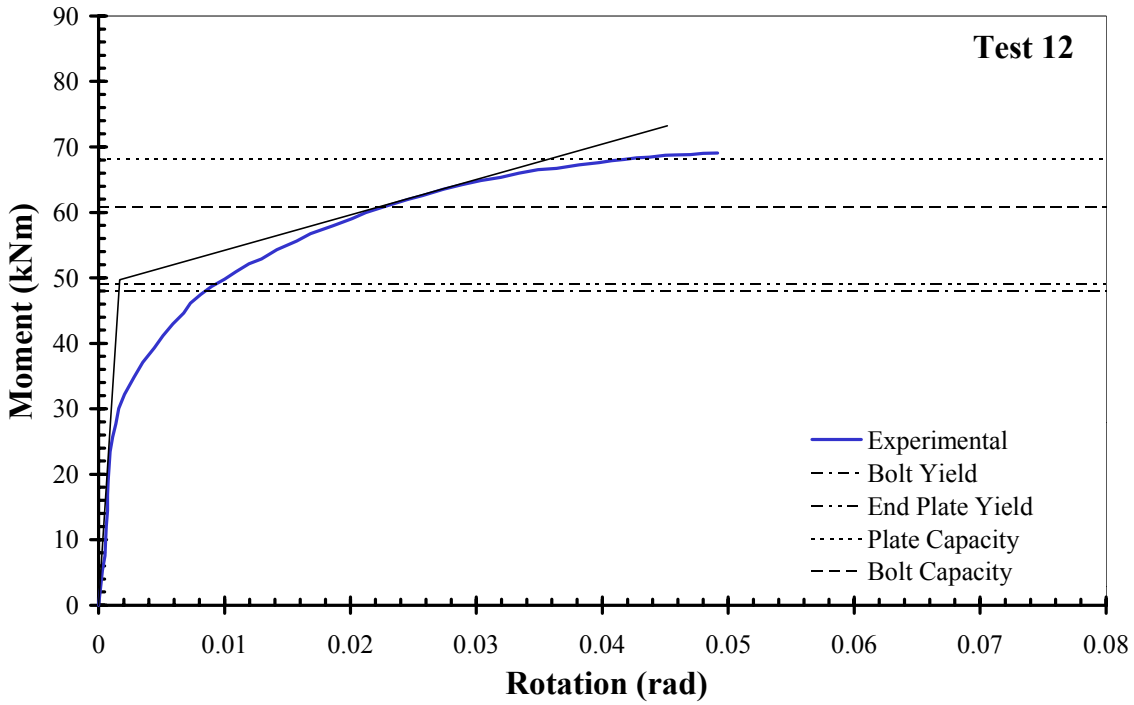

FIGURE B2 - Moment-rotation curve for Test 12
(SHS, W_p = 210 mm, t_p = 16 mm)

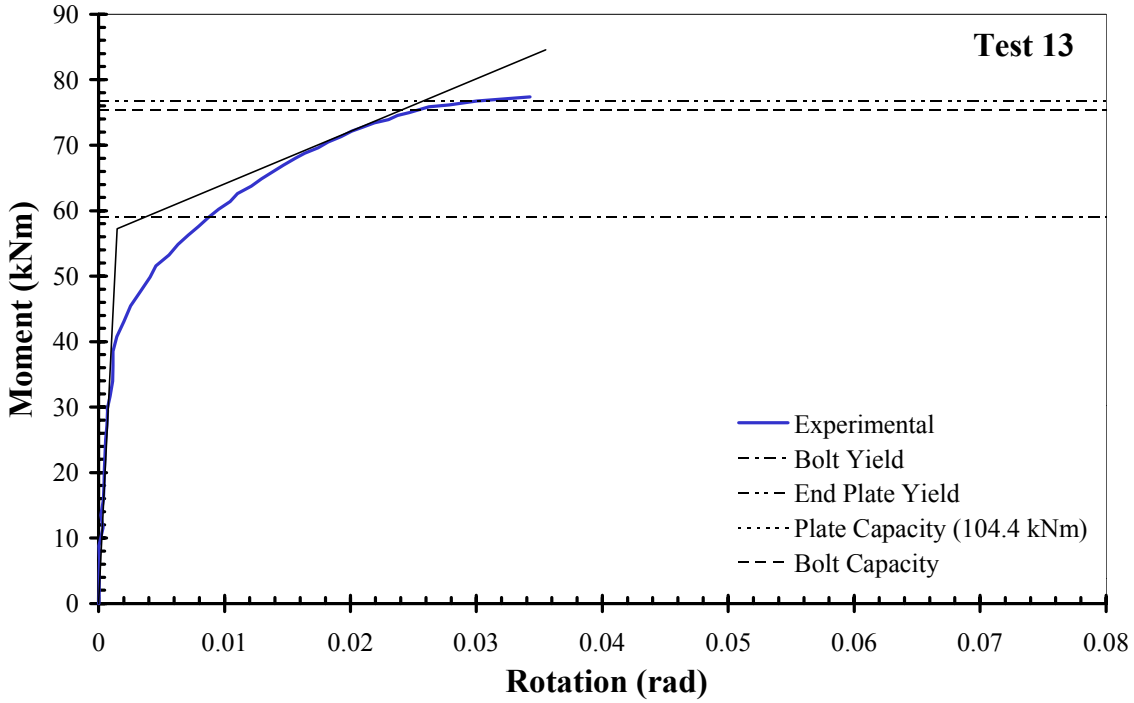

FIGURE B3 - Moment-rotation curve for Test 13
(SHS, W_p = 210 mm, t_p = 20 mm)

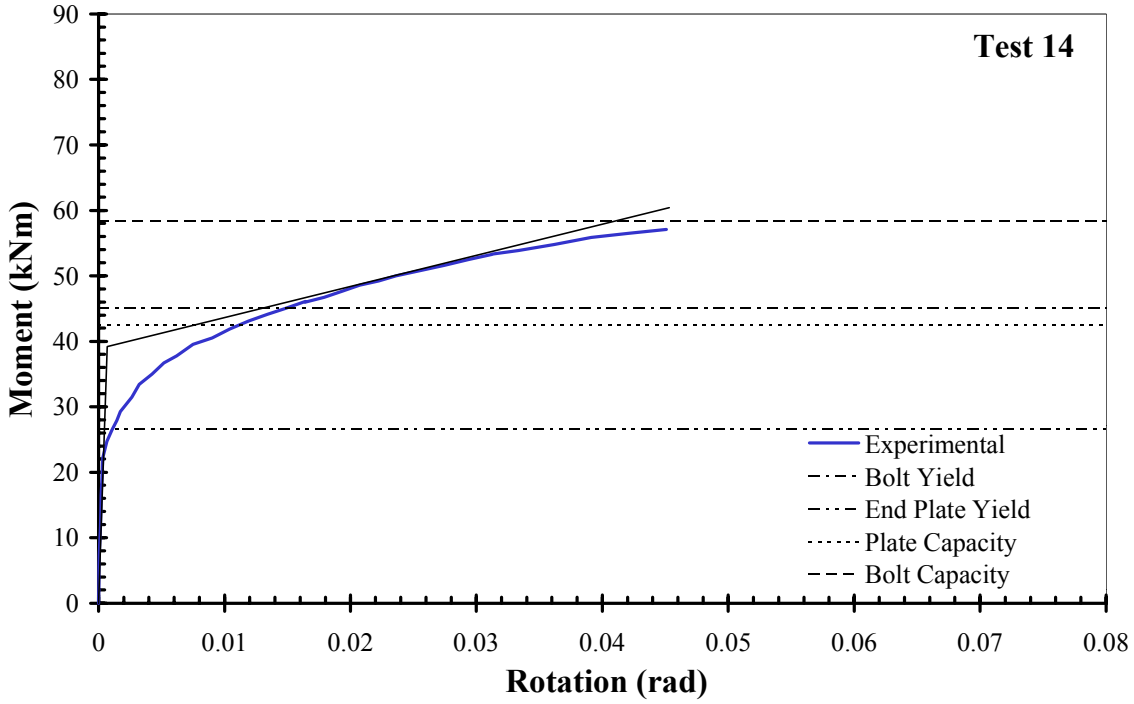

FIGURE B4 - Moment-rotation curve for Test 14, RHS
(W_p = 160 mm, t_p = 12 mm)

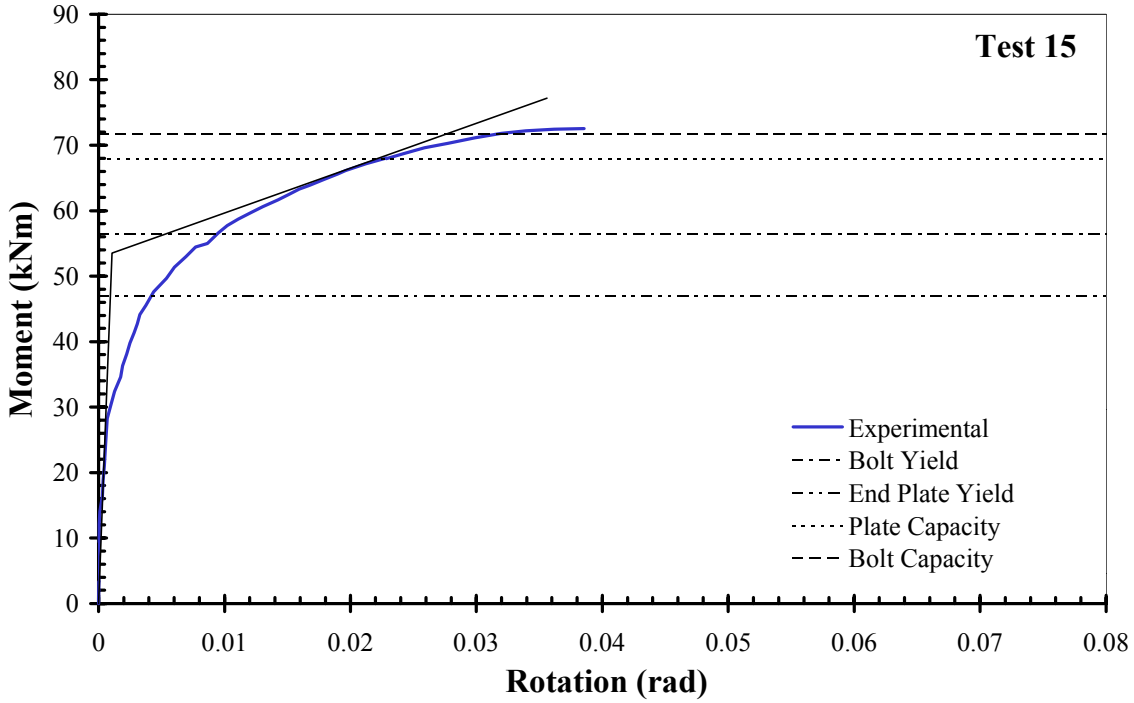

FIGURE B5 - Moment-rotation curve for Test 15
(RHS, W_p = 160 mm, t_p = 16 mm)

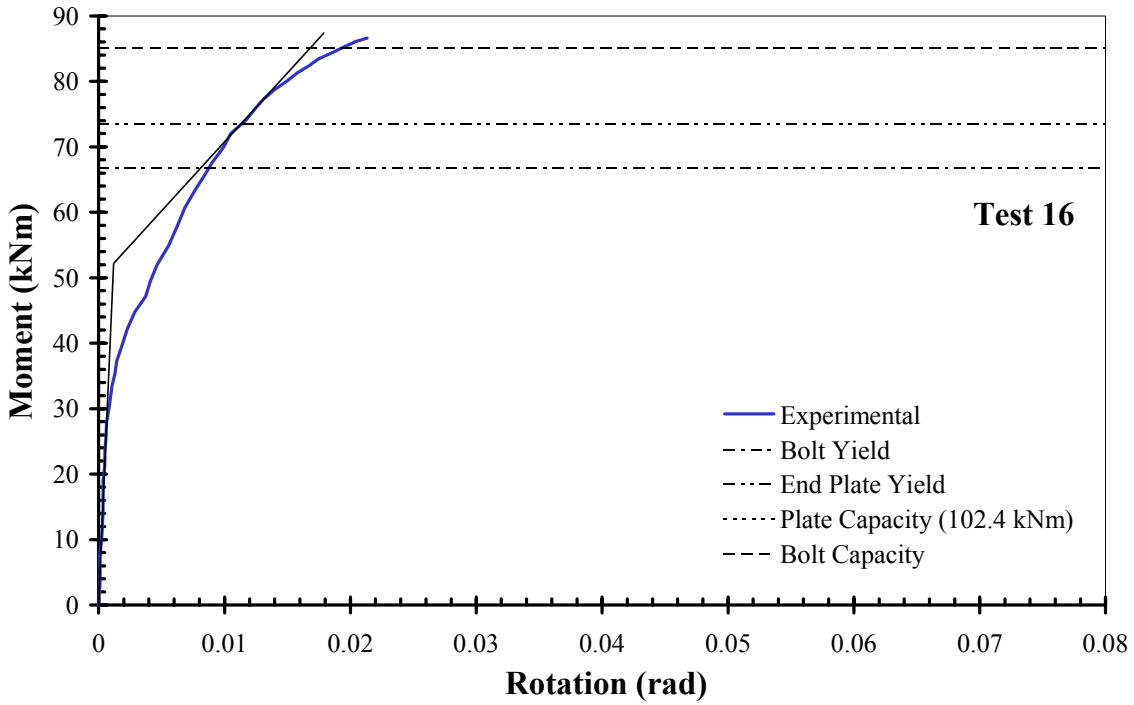

FIGURE B6 - Moment-rotation curve for Test 16
(RHS, W_p = 160 mm, t_p = 20 mm)

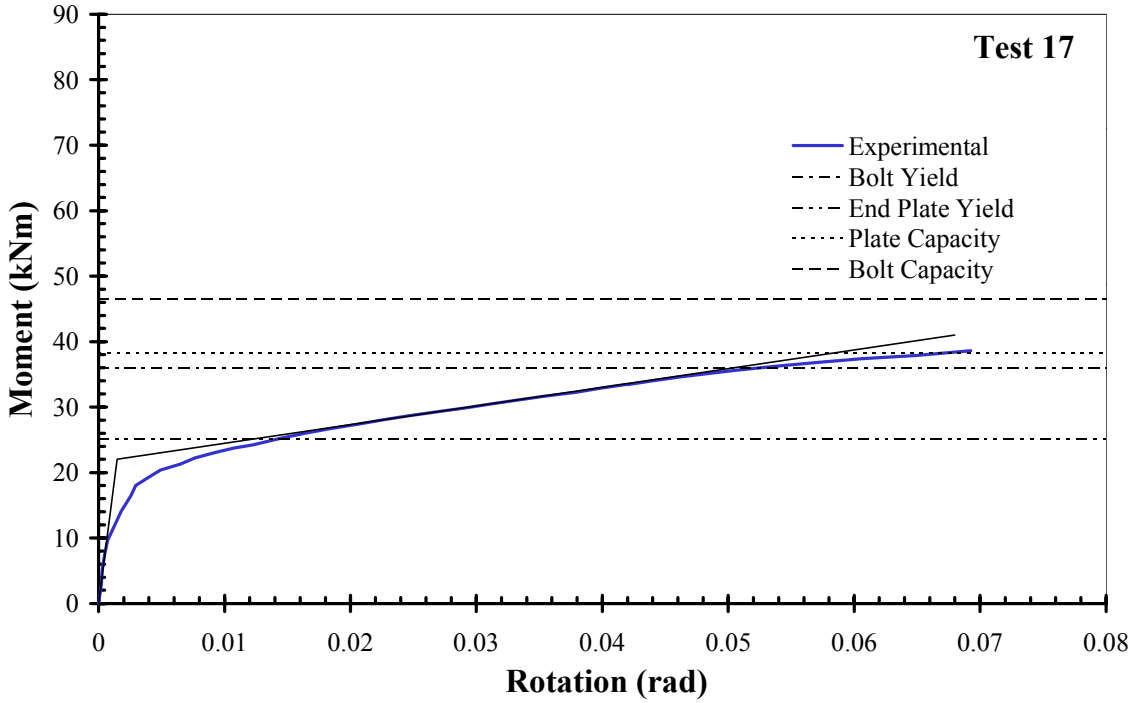

FIGURE B7 - Moment-rotation curve for Test 17
(SHS, W_p = 280 mm, t_p = 12 mm)

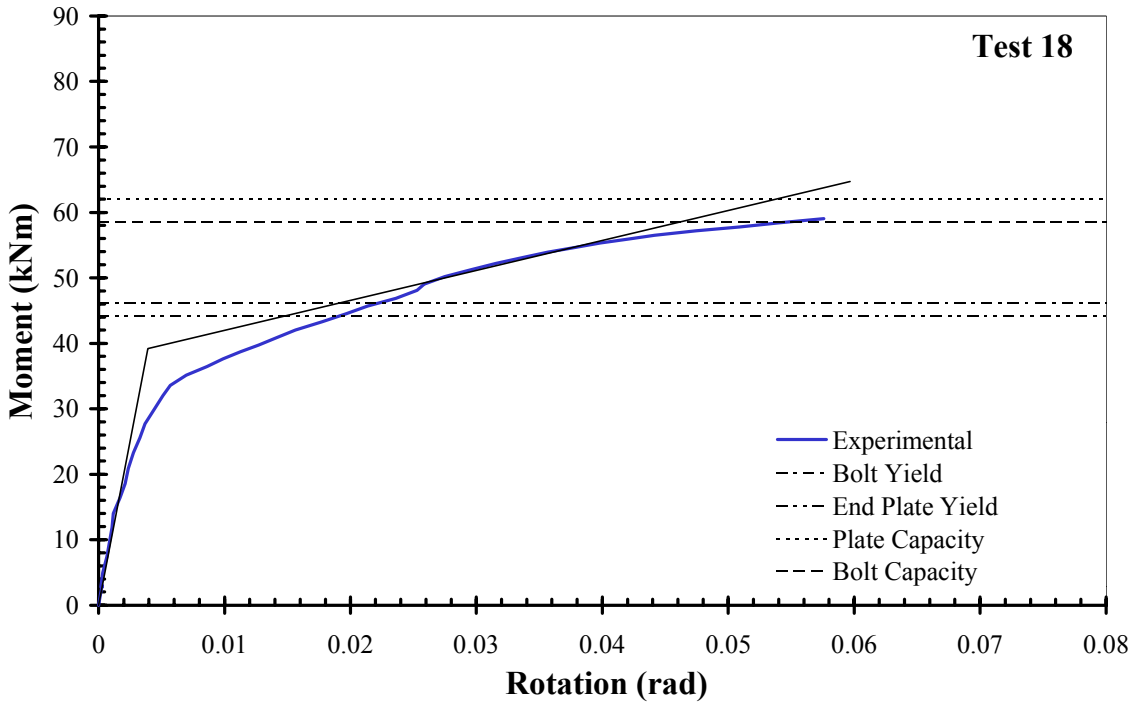

FIGURE B8 - Moment-rotation curve for Test 18
(SHS, W_p = 280 mm, t_p = 16 mm)

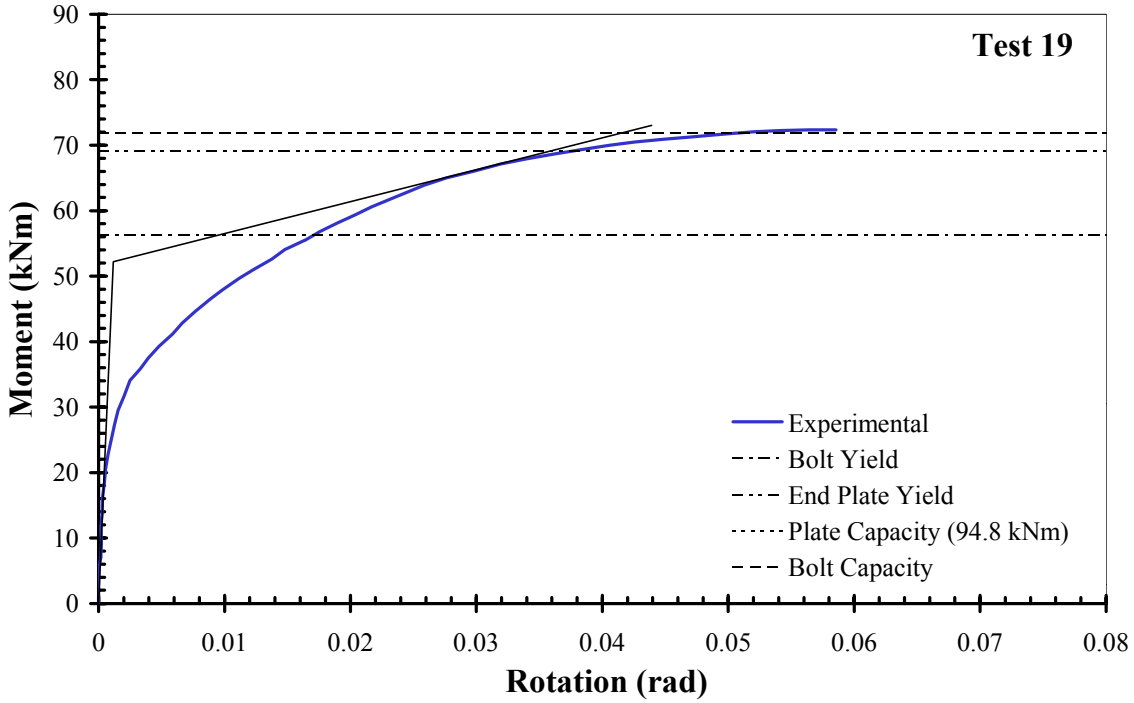

FIGURE B9 - Moment-rotation curve for Test 19
(SHS, W_p = 280 mm, t_p = 20 mm)

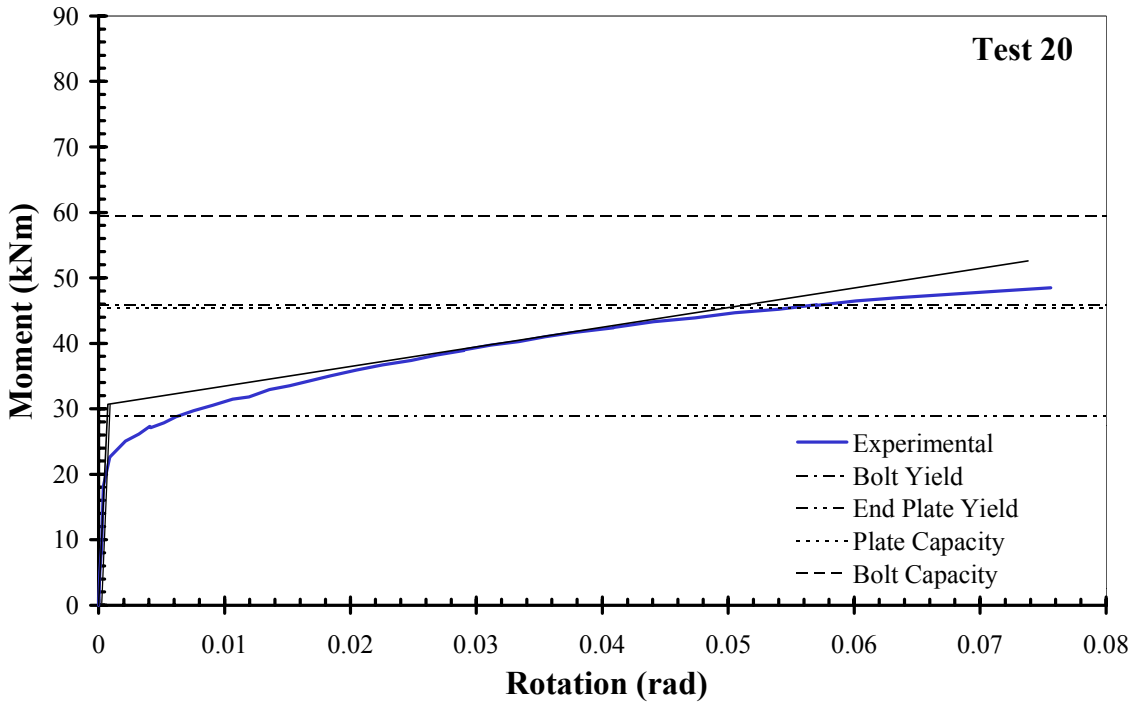

FIGURE B10 - Moment-rotation curve for Test 20
(RHS, W_p = 230 mm, t_p = 12 mm)

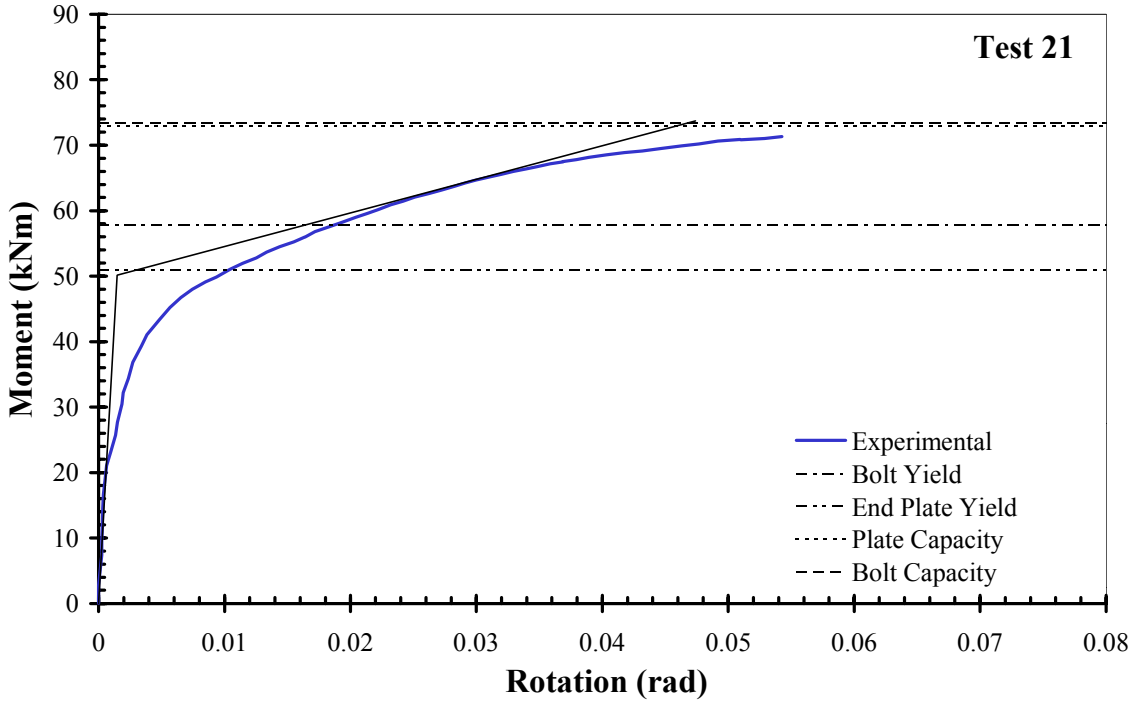

FIGURE B11 - Moment-rotation curve for Test 21
(RHS, W_p = 230 mm, t_p = 16 mm)

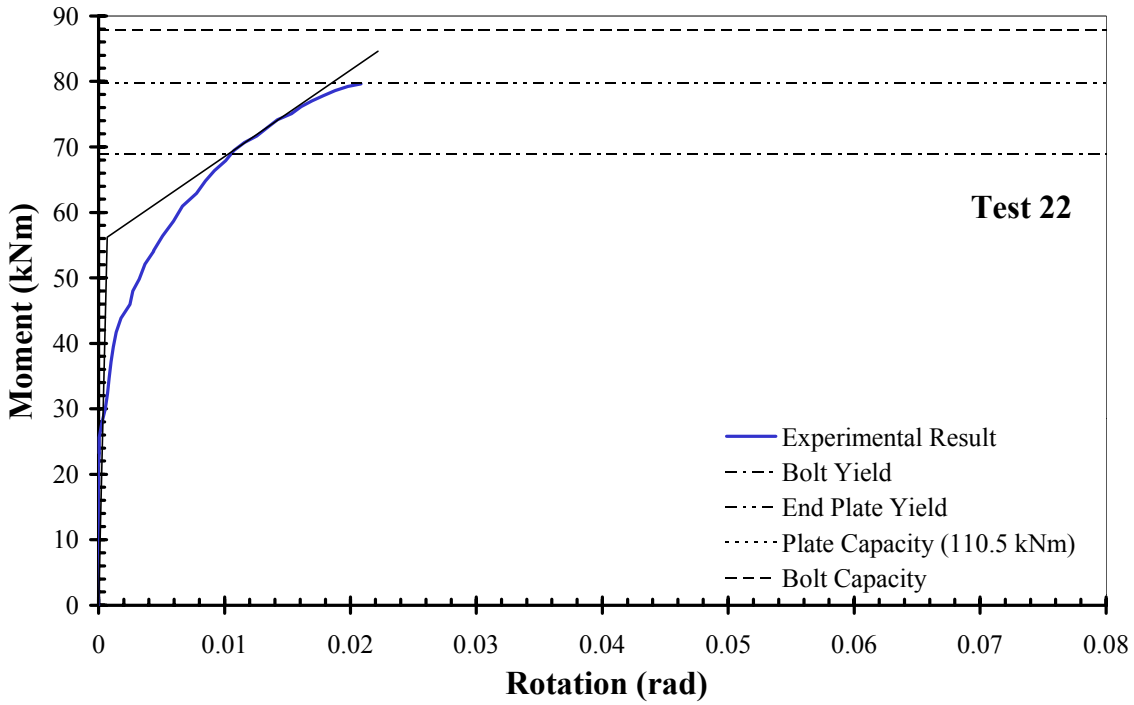

FIGURE B12 - Moment-rotation curve for Test 22
(RHS, W_p = 230 mm, t_p = 20 mm)

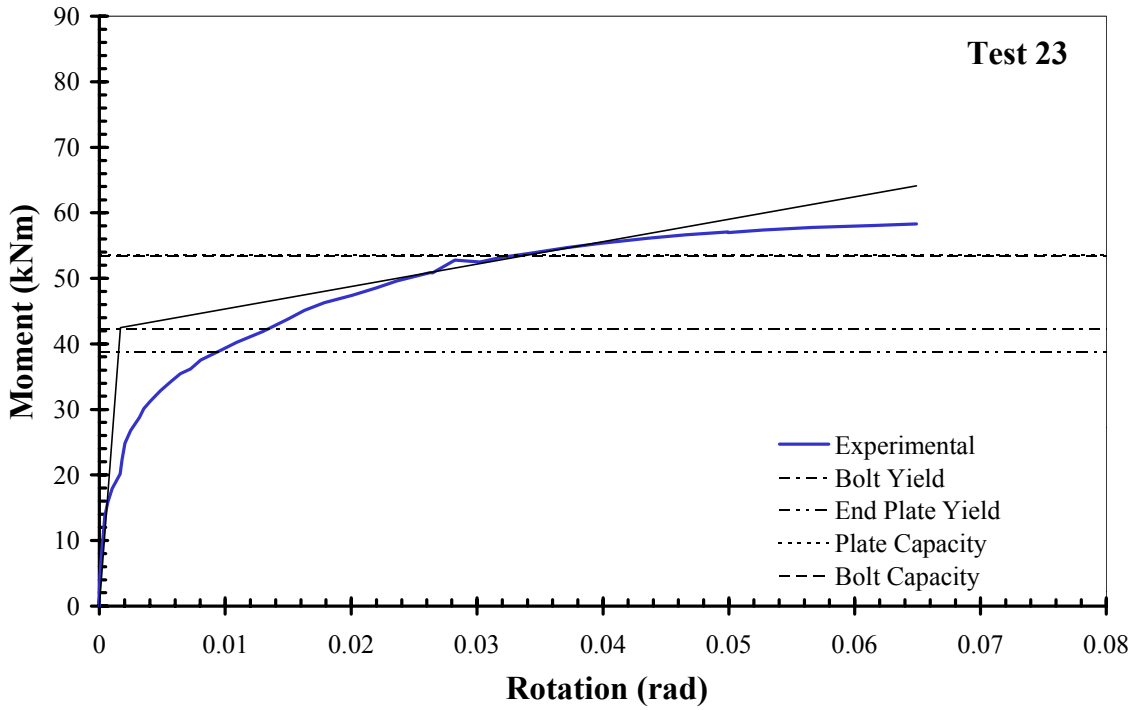

FIGURE B13 - Moment-rotation curve for Test 23
(SHS, W_p = 210 mm, t_p = 16 mm, s_o = 45 mm)

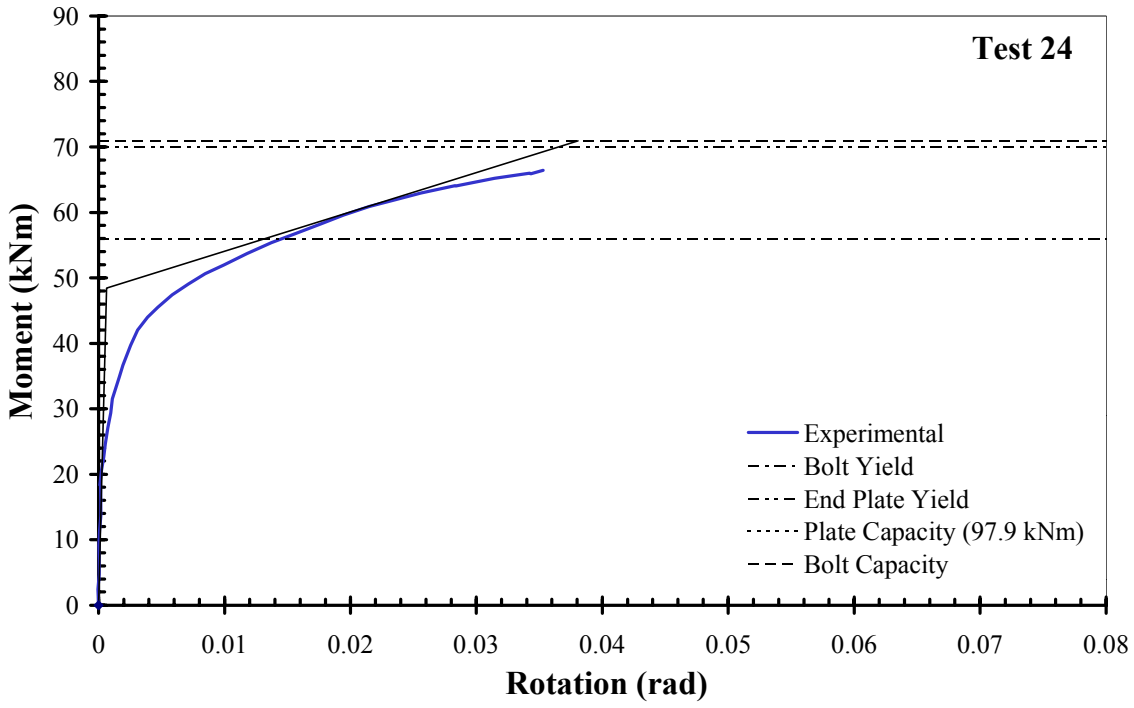

FIGURE B14 - Moment-rotation curve for Test 24
(SHS, W_p = 210 mm, t_p = 16 mm, s_o = 25 mm)

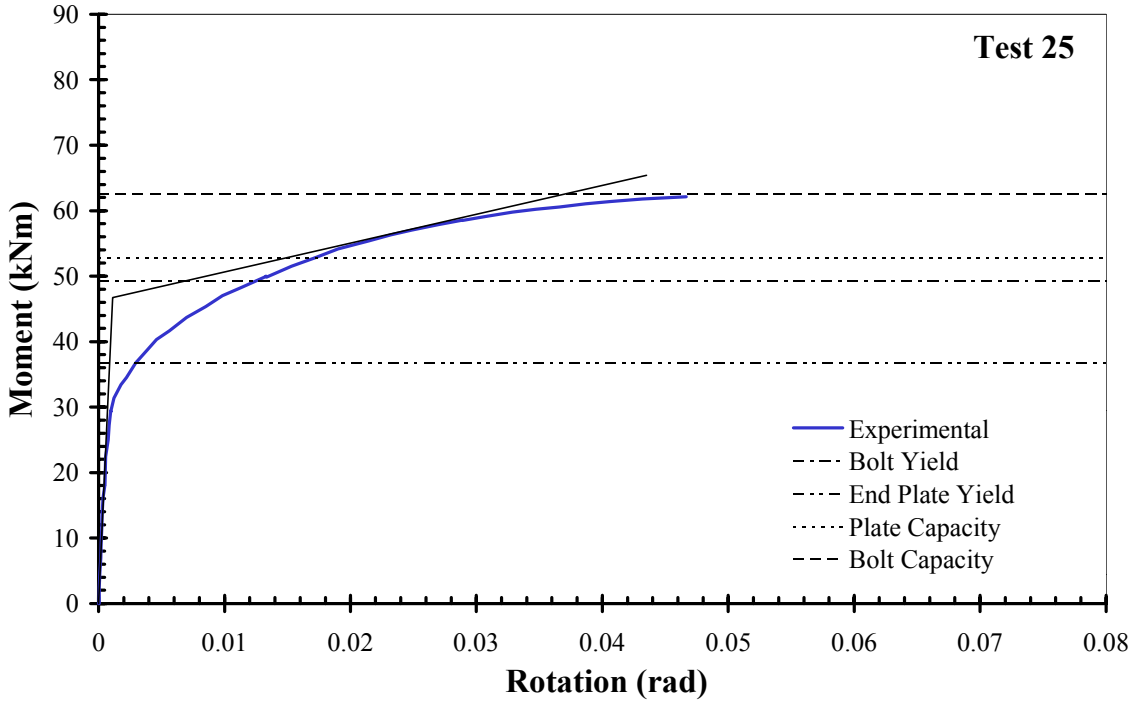

FIGURE B15 - Moment-rotation curve for Test 25
(SHS, W_p = 160 mm, t_p = 16 mm, s_o = 45 mm)

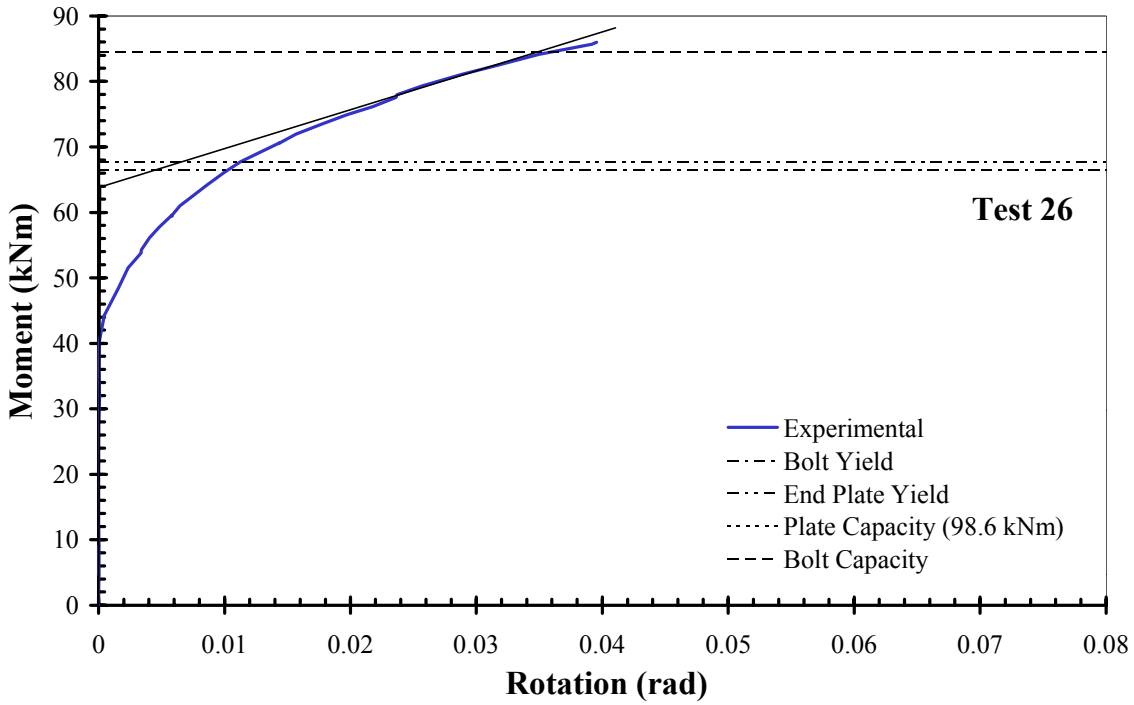

FIGURE B16 - Moment-rotation curve for Test 26
(RHS, W_p = 160 mm, t_p = 16 mm, s_o = 25 mm)